1-1-1977

A Model For Oxygen And Biomass Production In A Mass Algal Culture

F. P. Incropera

J. F. Thomas

TECHNICAL REPORT NO. 84

A MODEL FOR OXYGEN AND BIOMASS PRODUCTION IN A MASS ALGAL CULTURE

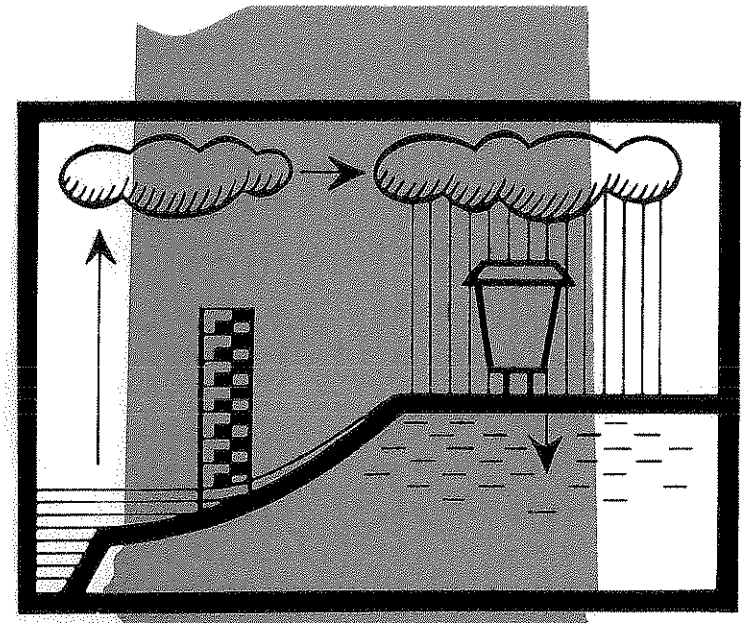

by

F.P. Incropera

J.F. Thomas

January 1977

PURDUE UNIVERSITY
WATER RESOURCES RESEARCH CENTER
WEST LAFAYETTE, INDIANA

A MODEL FOR OXYGEN AND BIOMASS PRODUCTION IN A MASS ALGAL CULTURE

by

F.P. Incropera

and

J.F. Thomas

The work upon which this report is based was supported in part by funds provided by the United States Department of Interior, Office of Water Research and Technology, as authorized by the Water Resources Research Act of 1964 (PL 88-379 as amended).

School of Mechanical Engineering

Purdue University

An interim report of OWRT Project No. A-042-IND
Period of Investigation: July 1, 1975 to June 30, 1978

Technical Report No. 84
Purdue University Water Resources Research Center
West Lafayette, Indiana 47907

January 1977

FOREWORD

The study reported in this document was supported by the U.S. Department of Interior, Office of Water Research and Technology as part of the annual allotment program for Purdue University Water Resources Research Center. Project personnel were Dr. Frank P. Incropera, principal investigator, and Mr. John Thomas, research assistant. Acknowledgment of support is given to Dr. Daniel Wiersma, Director of the Indiana Water Resources Research Center.

One of us (J.F.T.) gratefully acknowledges support received during the summer of 1975 under a National Science Foundation Undergraduate Research Participation Grant (EPP75-04328). The authors wish to acknowledge useful discussions with Doctor Kenneth J. Daniel concerning radiative transfer in algal suspensions.

LIST OF CONTENTS

ABSTRACT

In recent years there has been renewed interest in the mass culture of unicellular algae. Such cultures show considerable promise for augmenting biological wastewater treatment processes and for producing a high protein food supplement. In connection with such applications it would be useful to have reliable methods for predicting the yield of a mass culture as a function of geographic location and diurnal and seasonal conditions. Although some empirical correlations have been developed for this purpose, there is presently no method which systematically accounts for the relevant radiative and kinetic effects. The primary purpose of this study has been to develop a model which treats such effects and is able to predict the maximum hourly production of algae in a shallow pond.

The model determines both oxygen and algal biomass production and is based upon the use of available insolation data. It accounts for spectral effects in the photosynthetically active region, as well as directional effects through delineation of the diffuse and collimated components of the radiation. The effects of the air-water interface are treated, and predictions of the radiation field within the water are used with a representative photosynthesis model to predict the hourly yield. Calculations have been performed for the Indianapolis, Indiana region, and comparisons with field data for similar latitudes reveal that the model is well suited for predicting the maximum yield of mass cultures.

LIST OF TABLES

LIST OF FIGURES

LIST OF SYMBOLS

a', a''	atmospheric transmission coefficients
B	ratio of cell dry mass production to O_2 evolution, $mg(\text{dry mass algae}) \cdot mol(O_2)^{-1}$
C	cloud coverage in tenths
C_a	algal mass density, $mg(\text{dry mass algae}) \cdot m^{-3}$
C_c	integrated chlorophyll concentration defined by equation (52), $mg(\text{chlorophyll}) \cdot m^{-2}$
D	pond depth, m
d	dust depletion coefficient
F	solar irradiance, $\text{einstein} \cdot m^{-2} \cdot hr^{-1}$
F_λ	monochromatic solar irradiance, $\text{einstein} \cdot m^{-2} \cdot hr^{-1} \cdot nm^{-1}$
H_λ	monochromatic radiation absorption per unit volume, $\text{einstein} \cdot m^{-3} \cdot hr^{-1} \cdot nm^{-1}$
H_λ'	monochromatic radiation absorption per unit mass of chlorophyll, $\text{einstein} \cdot mg(\text{chlorophyll})^{-1} \cdot hr^{-1} \cdot nm^{-1}$
H_v'	radiation absorption per unit mass of chlorophyll for the visible region of the spectrum, $\text{einstein} \cdot mg(\text{chlorophyll})^{-1} \cdot hr^{-1}$
I_λ	monochromatic radiance, $\text{einstein} \cdot m^{-2} \cdot hr^{-1} \cdot nm^{-1} \cdot sr^{-1}$
$I_{\lambda,o}$	monochromatic radiance of the residual diffuse radiation at $\theta_i=0$, $\text{einstein} \cdot m^{-2} \cdot hr^{-1} \cdot nm^{-1} \cdot sr^{-1}$
$\bar{I}_v^d$	diffuse radiance for the visible region of the spectrum normalized with respect to the radiance at zero incidence ($\theta_i=0$)
m	relative air mass
n	refractive index of water
P_a	total rate of algal biomass production per unit pond surface area, $g(\text{dry mass algae}) \cdot hr^{-1} \cdot m^{-2}$
$\bar{P}_a$	daily algal biomass production per unit surface area of culture, $g(\text{dry mass algae}) \cdot d^{-1} \cdot m^{-2}$
P_o	total rate of oxygen evolution per unit surface area of culture, $mol(O_2) \cdot hr^{-1} \cdot m^{-2}$
$\bar{P}_o$	daily oxygen evolution per unit surface area of culture, $mol(O_2) \cdot d^{-1} \cdot m^{-2}$
P_λ	monochromatic phase function of algae
p_a	local net rate of algal biomass production, $mg(\text{dry mass algae}) \cdot hr^{-1} \cdot m^{-3}$
p_a'	local net rate of algal biomass production, $mg(\text{dry mass algae}) \cdot hr^{-1} \cdot mg(\text{chlorophyll})^{-1}$
p_o'	local net rate of oxygen production,

	$mol(O_2) \cdot hr^{-1} \cdot mg(chlorphyll)^{-1}$
R	local rate of oxygen evolution, $mol(O_2) \cdot hr^{-1} \cdot mg(chlorophyll)^{-1}$
R_A	light dependent component of the local rate of oxygen evolution, $mol(O_2) \cdot hr^{-1} \cdot mg(chlorophyll)^{-1}$
R_M	kinetic constant, $mol(O_2) \cdot hr^{-1} \cdot mg(chlorophyll)^{-1}$
R_S	local rate of oxygen evolution for light saturated conditions, $mol(O_2) \cdot hr^{-1} \cdot mg(chlorophyll)^{-1}$
r_c	mass fraction of chlorophyll, mg(chlorophyll)·mg(dry mass algae)$^{-1}$
S	percent sunshine factor
$\bar{S}$	monthly average percent sunshine
T	pond temperature, K
t	time, hr
U	oxygen uptake due to respiration, $mol(O_2) \cdot hr^{-1} \cdot mg(dry\ mass\ algae)^{-1}$
w	atmospheric moisture content, cm
z	vertical distance in culture, m
α_λ	monochromatic absorption coefficient of algae, m^{-1}
β_λ	monochromatic extinction coefficient of algae, m^{-1}
β_λ'	modified extinction coefficient, $m^2 \cdot mg(chlorophyll)^{-1}$
η	efficiency for conversion of solar radiation to algal biomass
θ	zenith angle, degrees
λ	wavelength, nm
μ	specific growth rate, day^{-1} or hr^{-1}
ρ	reflectivity of the air-water interface
σ_λ	monochromatic scattering coefficient of algae, m^{-1}
τ	transmissivity of the air-water interface
ϕ	azimuthal angle, degrees and quantum yield, $mol(O_2) \cdot einstein^{-1}$
ϕ_λ	monochromatic quantum yield, $mol(O_2) \cdot einstein^{-1}$
Ω	solid angle, sr

Subscripts

c	clear day
i	incident solar radiation
o	extraterrestrial solar radiation
r	refracted solar radiation
S	light saturation

t	total radiation ($0 \leq \lambda \leq \infty$)
v	visible (PhAR) region of spectrum ($380 \leq \lambda \leq 720$ nm)
λ	monochromatic
$\Delta\lambda$	spectral bandwidth (10 nm)

Superscripts

C	effective collimated radiation
c	collimated radiation
D	residual diffuse radiation
d	diffuse radiation

CHAPTER 1 INTRODUCTION

1.1 Applications of Algae

Since the early nineteen fifties there has been considerable interest in the use of unicellular algae as a major source of food and chemicals. As a food source, the mass algal culture offers several advantages over conventional agriculture. Since unicellular algae has a high specific growth rate, can be cultured continuously throughout the year and has a minimum of structural material, yearly biomass production per unit area may be up to an order of magnitude larger than that associated with agronomic crops. Moreover, the protein content of algae is typically in excess of 50 percent, rendering the annual protein production of mass algal cultures as much as twenty-five times that of cereals and legumes. Actual field performance data for protein production have been reported as 1.57 $kg \cdot m^{-2} \cdot yr^{-1}$ for Chlorella pyrenoidosa [1] and from approximately 1 to 5 $kg \cdot m^{-2} \cdot yr^{-1}$ for unicellular algae cultured from organic wastes [2].

From a nutritional point of view the high protein and vitamin content of algae has stimulated considerable interest in its use as a food source. Numerous feeding trials have been performed, and recent reviews of the literature [3,4] suggest that, when properly processed, unicellular green algae provides a suitable protein source for animals and humans. Moreover, many useful chemical products may be recovered from algae [5], and algal fermentation systems may be used for the production of methane [6,7].

The algal culture may also be used to enhance waste water treatment. The use of symbiotic cultures of algae

and bacteria for sewage treatment has been extensively studied by Oswald [6-8]. Algae growth will release oxygen which can be used by aerobic bacteria in combined secondary-tertiary treatment ponds to reduce the biochemical oxygen demand (BOD) of the soluble organic matter. Water treatment is also effected through the assimilation of dissolved nutrients (nitrogen, phosphorus, etc.) by the algae. Moreover, bacterial decay of the organic matter releases carbon dioxide, which is also needed to sustain algal growth. This coupling of algal and bacterial growth processes therefore serves two useful and complementary purposes: (i) water quality is enhanced through BOD and nutrient removal and (ii) the economic aspects of algal biomass production become more favorable, since the required nutrients and carbon dioxide are obtained by recycling organic waste materials. More recently, the foregoing process has been extended to the reclamation of agricultural wastes [9].

1.2 Factors Influencing Algal Growth

Algal growth occurs through photosynthesis, and under field conditions the energy required for the process is derived exclusively from solar radiation. The intensity of this radiation has a strong influence on the production and operational parameters of the algal system. The spectral range of the radiation used by the algae (the photosynthetically active region) is from 380 to 720 nm, and the maximum efficiency of energy utilization amounts to approximately 20 percent of the radiation in this range [10], or approximately 8 percent of the total solar radiation [9]. However, maximum efficiencies have only been approached in carefully controlled laboratory cultures. In mass algal cultures the efficiency with which solar energy is converted to the chemical energy of algal biomass is somewhat lower, generally ranging from 1 to 3 per-

cent. These lower energy conversion efficiencies are due to the fact that numerous variables influence the rate of photosynthesis and that, under most conditions, the process is light saturated.

In addition to the intensity of the visible radiation, the independent variables which determine the local photosynthesis rate, and hence the performance of an algal culture, are the CO_2 concentration, the nutrient (mineral) concentrations, the specific growth rate and the temperature [11]. The rate of CO_2 transport across the air-water interface is insufficient to sustain a rapidly growing algal culture; however if there is an internal source of CO_2 (due to mechanical injection and/or symbiotic conditions), algal growth will not be CO_2 limited.

The minerals required for algal growth include macronutrients such as nitrogen, phosphorus, sulfur and potassium and micronutrients such as zinc, manganese and copper. Although one or more of these elements may be growth-limiting in an outdoor culture, the limitations may be eliminated through nutrient control. For example, the concentration of nitrogen may become limiting if algae is cultured exclusively from a nutrient medium consisting of domestic sewage [12], but the limitation may readily be removed with nitrogen supplementation from some other source. In contrast, animal manure provides a highly concentrated source of minerals for which none of the macro or micronutrients are likely to be limiting [9].

Algal production is also influenced by the specific growth rate, which is simply the rate of growth of the algae ($kg \cdot m^{-3} \cdot hr^{-1}$) relative to the algae concentration ($kg \cdot m^{-3}$). Because this quantity can significantly influence the response of algae to temperature, the intensity of visible radiation, and to the CO_2 and nutrient concentrations, it must be treated as an independent variable [11].

The temperature dependence of algal growth originates from its effect on the rate of the enzyme catalyzed biochemical reactions which comprise the photosynthesis process. The effect of temperature on the growth rate of C. pyrenoidosa has been studied [1,12,13], and growth rate has been found to increase with increasing temperature up to approximately 298 K and 312 K, respectively, for mesophilic and thermophilic strains. The effect is particularly significant for the thermophilic strains, whose doubling rates are known to increase nearly fivefold for a temperature increase from 293 to 312 K. Accordingly, the use of temperature control to maintain maximum algal growth conditions is highly desirable, and it has been advocated that the waste heat from electrical power plants be used for the purpose of implementing this control [9,14]. In fact, it was recently concluded that, for most regions of the earth, the availability of waste heat was necessary for the production of algae in an economically viable manner [15].

From the foregoing discussion it is evident that, in the interest of maximizing algal production, rate limitations due to temperature and CO_2 and nutrient concentrations should be eliminated. The control over growth conditions required to achieve this objective may be effected economically by relying on symbiotic cultures, which use domestic and/or animal wastes as a substrate, and the use of powerplant waste heat to maintain yearround optimum culture temperatures. In this study it is assumed that such control is exercised, in which case the only limitations on algal production are due to the availability of solar radiation and the specific growth rate of the algae.

1.3 Objectives of this Study

The primary objective of this study is to formulate a model which may be used to assess the influence of solar irradiance on the production of mass algal cultures. In

particular, a model is formulated which assumes the availability of solar radiation to be the major growth-limiting factor. The model is based upon current knowledge of the kinetics of photosynthesis and of solar radiation transfer in an algal suspension. It may be used to predict the seasonal variation of biomass and oxygen production for different geographic locations and to determine optimum design and operating conditions for mass cultures. It therefore provides a useful tool for determining the feasibility of using solar energy to produce single cell protein and to enhance water quality through the reduction of BOD and nutrient content.

CHAPTER 2 THE KINETIC MODEL

2.1 Preliminary Remarks

To model the performance of an optically dense algal culture, it is necessary to know the distribution of the radiation field within the culture and to have a suitable kinetic model for relating the rate of photosynthesis to the irradiance. The local rate of photosynthesis may then be determined for any point in the culture, and the results may be integrated over the entire culture volume to determine the total rate of algal biomass and oxygen production. In this chapter various kinetic models are reviewed for the purpose of selecting the most representative formulation of the photosynthesis process. In the following chapter procedures are developed for computing the distribution of solar radiation in a dense algal culture. The kinetic and radiative transfer models are then coupled for the purpose of predicting total culture production.

There are, of course, many different species of unicellular algae, with each species characterized by a unique set of kinetic parameters. However, this study will focus on the particular species Chlorella pyrenoidosa. In addition to being an algal form whose kinetics have been widely considered [1,11,12], it occurs commonly in natural systems, as well as in mass cultures. Moreover, many of its characteristics are similar to those of other common species of green algae, such as Scenedesmus and C. vulgaris, and it grows readily on nutrient media comprised of animal and human wastes.

2.2 Review of Existing Models

An important step in the development of rational methods

for predicting the performance of algal cultures involved the use of an overall light or energy conversion efficiency for photosynthesis [16]. Algal growth was assumed to be determined exclusively by the availability of visible radiation, and an overall conversion efficiency was used to relate growth to the local irradiance. However, although the method has been used to estimate the production of laboratory and mass cultures [9,12], it remains somewhat approximate. In addition to relying on empirical light conversion efficiencies which are not generally applicable, it is unable to systematically treat the effects of saturating light intensities.

Numerous experimental studies have been performed in an effort to better correlate the effect of the photosynthetically active irradiance on algal growth. The studies have led to the development of light response curves which describe the rate of photosynthesis as a function of the irradiance. The simplest model is one which assumes a linear variation of the photosynthesis rate with irradiance up to a maximum rate corresponding to saturated conditions. The photosynthesis rate remains constant at the maximum value for any increase in irradiance beyond saturation. Alternative formulations involve fitting the light response curve by rectangular hyperbola and exponential functions.

Unfortunately, there is no general agreement on which of the foregoing models provides the best representation of algal growth conditions. The data of Sorokin and Krauss [17] support the linear model, while the results of Tamiya [1] have consistently corroborated the rectangular hyperbola. In contrast other experimental results [12,18,19] are better correlated in terms of the exponential function.

Despite the existence of supporting data for each of the foregoing models, at least two factors contribute to the failure of each model to provide a generally applicable correlation of photosynthesis data. One limitation relates to the fact that the models are highly empirical and do not

reflect the kinetic mechanisms which are presently thought to determine photosynthesis. The exponential model is completely without theoretical basis, and the linear and rectangular-hyperbola models may be derived only by assuming highly simplified kinetic mechanisms [12]. A more serious problem is the fact that none of the models account for the effect of algal physiology on the light response curve. In particular algal growth conditions can strongly influence the cell chlorophyll content and respiration rate, which in turn affect net photosynthesis.

In a more recent study [11] the foregoing limitations were considered, and attempts were made to develop an improved model for the light dependence of photosynthesis. Although present knowledge of the kinetic mechanisms which comprise the photosynthesis process is incomplete, much has been learned about the nature of the light reactions and the photo-electron transport system. Dabes et al. [11] have developed a kinetic model which is consistent with the current view of photosynthesis. In particular it accounts for the existence of two light reactions, and it assumes that the rate limiting step (which determines the light saturated rate of photosynthesis) is a reaction in the carbon fixation cycle which affects the generation of ATP. Moreover, the model attempts to account for the effect of algal physiology through its inclusion of the specific growth rate as an independent variable. The specific growth rate μ is simply a measure of the rate of growth of new algae relative to the existing algal mass

$$\mu \equiv \frac{1}{C_a} \frac{dC_a}{dt} \qquad (1)$$

Although the photosynthesis rate is independent of μ at low values of the irradiance, a strong dependence is known to exist at high irradiance [11] and should be included in the kinetic model.

2.3 Formulation of the Model

The kinetic model of Dabes et al. [11] has been selected for use in this study. The model provides an expression for the local rate of photosynthesis in terms of the oxygen evolution. If the local irradiance is less than saturating, the oxygen evolution may be expressed as

$$R(z,\mu) = \frac{2R_A R_M}{2R_M + R_A + (2R_A R_M + R_A^2)^{1/2}} \qquad (2)$$

If the local irradiance exceeds the saturating value, the oxygen evolution is

$$R(\mu) = R_S \qquad (3)$$

Under the nonsaturating conditions of (2) the local rate of photosynthesis, which has units of $mol(O_2) \cdot hr^{-1} \cdot mg(chlorophyll)^{-1}$, depends upon the specific growth rate μ and the depth z within the culture through the variation of the irradiance with μ and z. This dependence originates from the term R_A, which may be expressed as

$$R_A = \int_{380}^{720} \frac{\phi_\lambda(\lambda)}{C_a r_c} H_\lambda(z,\lambda)\, d\lambda \qquad (4)$$

where ϕ_λ is the monochromatic quantum yield, expressed in terms of the number of moles of O_2 released relative to the number of moles (einsteins) of radiation absorbed. The absorbed radiation, H_λ, is measured in units of $einstein \cdot m^{-3} \cdot hr^{-1} \cdot nm^{-1}$ and varies with position in the culture. The means by which it may be determined are described in Chapter 3. The product $C_a r_c$ converts from oxygen evolution per unit volume to oxygen evolution per unit mass of chlorophyll. Note, that under the saturating

conditions of (3), the local rate of photosynthesis is independent of depth. However, because growth conditions may still influence the dependence of photosynthesis on irradiation at saturation, the dependence on μ is retained.

From a comparison of (2) with experimental results obtained for the variation of photosynthesis rate with non-saturating values of the irradiance [11], it was found that the dependence of ϕ_λ on λ could be neglected and that values of $\phi_\lambda = \phi = 0.1138$ mol(O_2)·einstein^{-1} and $R_M = 2.21 \times 10^{-3}$ mol(O_2)·hr^{-1}·mg (chlorophyll)$^{-1}$ adequately correlated the data. In addition from measurements of the variation of saturating photosynthesis rate with specific growth rate, the following correlation was found to be appropriate for R_S

$$R_S = 1.174 \times 10^{-4} + 1.334 \times 10^{-4} \mu \qquad (5)$$

where μ is in units of day^{-1}.

Oxygen evolution due to photosynthesis is, of course, related to algal biomass production, and it is possible to convert from one to the other. The specific form of the conversion depends upon growth rate, and the following correlation has been obtained for the ratio of cell biomass production to oxygen evolution [11]

$$B = 1.64 \times 10^{4} + 0.065 \times 10^{4} \mu \qquad (6)$$

where the units of B are mg(dry mass algae)·mol(O_2)$^{-1}$ and μ is in day^{-1}. It should also be noted that (2) and (3) pertain to gross photosynthesis and do not account for losses associated with respiration. The rate at which oxygen is consumed in respiration also depends on growth conditions and may be correlated by an expression of the form

$$U = 7.81 \times 10^{-8} + 2.18 \times 10^{-4} \mu \qquad (7)$$

where the units of U are $mol(O_2) \cdot hr^{-1} \cdot mg(\text{dry mass algae})^{-1}$ and μ is again in day^{-1}. Finally, we note that (2) and (3) provide the rate of photosynthesis per unit mass of chlorophyll. To convert to photosynthesis per unit mass of dry algae, it is only necessary to multiply by the mass fraction of chlorophyll in the algal cells, which is a known function of specific growth rate [11]

$$r_c = 7.43 \times 10^{-2} - 2.61 \times 10^{-2} \mu \tag{8}$$

where r_c is in units of $mg(\text{chlorophyll}) \cdot mg(\text{dry mass algae})^{-1}$.

The foregoing model may be used as a basis for determining the total oxygen evolution and biomass production for an algal culture. However, one complicating feature of the model should be noted. Because of its influence on algal physiology and hence algal kinetics, the specific growth rate has been treated as an independent variable. However, the specific growth rate is also directly related to the principal dependent variable, namely the net algal production. This relation is evident from the following expression for the local net rate of production of algal biomass

$$p_a = \frac{dC_a}{dt} = C_a [R(\mu,z)B(\mu)r_c(\mu) - U(\mu)B(\mu)] \tag{9}$$

where p_a has units of $mg(\text{dry mass algae}) \cdot hr^{-1} \cdot m^{-3}$. From (1) the local specific growth rate is then

$$\mu = R(\mu,z)B(\mu)r_c(\mu) - U(\mu)B(\mu) \tag{10}$$

in which case

$$p_a = C_a \mu \tag{11}$$

The dual role played by μ as both a dependent and an

independent variable will necessitate an iterative solution to the kinetic model.

The total productivity per unit surface area of the culture P may be obtained by integrating (11) over the culture depth. Hence, if the culture is well mixed, such that C_a is independent of z,

$$P_a = C_a \int_0^D \mu \, dz \tag{12}$$

or

$$P_a = C_a \bar{\mu} D \tag{13}$$

where $\bar{\mu}$ is the spatial average value of the specific growth rate

$$\bar{\mu} \equiv \frac{1}{D} \int_0^D R(\mu,z) B(\mu) r_c(\mu) dz = U(\mu) B(\mu) \tag{14}$$

The rate of oxygen evolution per unit surface area of the culture may then be approximated as

$$P_O = P_a / B(\bar{\mu}) = (C_a \bar{\mu} D) / B(\bar{\mu}) \tag{15}$$

The foregoing model provides a comprehensive description of algal production in a mass culture. In addition to accounting for the spectral dependence of the photosynthetically active radiation, it uses a light response curve which is consistent with the contemporary view of photosynthesis. It also accounts for the effect of specific growth rate on the cellular chlorophyll content, the respiration rate, the saturated photosynthesis rate, and the relationship of oxygen evolution to algal biomass production. However, as previously mentioned, treatment of μ as an independent variable, while simultaneously acknowledging its relationship to algal production, necessitates

the use of an iterative solution procedure. The following procedure was used for the calculations of this study.

(i) For a prescribed form of the insolation and a specific value of the algal concentration C_a, a trial value of the average specific growth rate $\bar{\mu}$ is selected.

(ii) Assuming that μ does not vary with position in the culture, which is reasonable for well mixed conditions, $\mu=\bar{\mu}$ and the coefficients $r_c(\bar{\mu})$, $U(\bar{\mu})$, $R_s(\bar{\mu})$ and $B(\bar{\mu})$ may be determined.

(iii) From procedures to be described in the following section, the variation of the irradiance with depth is computed and the results are used to determine $R(z,\mu)$ from (2) or (3).

(iv) The value of $\bar{\mu}$ is then determined from (14) and compared with the trial value from step (i). The process is repeated until the computed and trial values of $\bar{\mu}$ agree to within 1 percent.

(v) Once convergence upon the correct value of $\bar{\mu}$ is obtained, the culture biomass production and oxygen evolution are computed from (13) and (15), respectively.

The above procedure was used by Dabes et al. [11] to predict the performance of a dense laboratory culture of C. pyrenoidosa. However, it was found that, for a broad range of specific growth rates, the theory consistently overpredicted the experimental results by 16%. Moreover, it was not possible to determine the specific source of the discrepancy. It was therefore decided to use the model in its present form but to reduce the computed results for oxygen evolution and algal biomass production by 16%. Hence, in the calculations of this study, a correction factor of 0.84 is applied to equation (13).

Finally, it should be remembered that the foregoing model is based on the assumption that neither the nutrient concentrations nor the temperature are limiting. Nevertheless, the empirical coefficients used in the model were

inferred from laboratory experiments conducted at 298 K [11]. Hence it is useful to consider in what way the model could be modified to determine the productivity of cultures which are maintained at temperatures other than 298 K. From experiments performed for various strains of C. pyrenoidosa [1,11,12,13], there is no doubt that temperature can have a significant influence on biomass production and oxygen evolution. This influence is manifested through the dark (enzyme) reactions which provide for the fixation of CO_2 in the photosynthesis process, and it becomes more important for irradiances close to saturation. The data suggest that, for the thermophilic forms of algae and for light intensities near saturation,[+] the growth rate increases nearly linearly with temperature up to a maximum which occurs at approximately 312 K [1,11,13]. The data of Dabes et al. [11] further suggest that the effects of temperature may be modelled exclusively through the term R_S for the rate of photosynthesis under light saturated conditions. Accordingly, it is suggested that the effects of temperature may be included by applying a correction factor to (5). For thermophilic strains of C. pyrenoidosa and the range $283 \leq T \leq 312°K$, the following expression is recommended as a first approximation

$$R_S(\mu,T) = (0.04667T-12.9076)(1.174+1.334\mu)x10^{-4} \qquad (16)$$

where T is in K and μ has units of day^{-1}.

[+] There appears to be little or no effect of temperature, at the lower, nonsaturating values of the irradiance [11].

CHAPTER 3. THE RADIATION MODEL

The problem of predicting algal growth now reduces to one of determining the variation of the solar irradiance with depth in the pond. The problem has three components which may be considered separately. They include (i) determination of the spectral and angular distribution of the solar radiation incident on the pond surface, (ii) determination of the reflection and refraction of this radiation at the air-water interface and (iii) determination of the radiation transfer within the pond itself.

3.1 The Incident Solar Radiation

Solar radiation reaching the surface of an algal pond is comprised of collimated and diffuse components (Fig. 1). All of the collimated, or direct, radiation is incident at a well defined angle; whereas the diffuse radiation, which originates from atmospheric scattering, is distributed over all directions. To predict algal growth within the pond, it is necessary to know the direction θ_i^c and the spectral distribution $F_\lambda^c(\lambda)$ of the monochromatic irradiance for the collimated radiation. It is also necessary to know the spectral and directional distribution of the monochromatic radiance, $I_\lambda^d(\theta_i,\phi_i,\lambda)$ for the diffuse radiation.

The incident angle of the collimated radiation (the solar zenith angle) varies with time of day, time of year and geographic location and may be determined from standard methods [20]. However, the directional distribution of the diffuse component is highly variable, depending upon atmospheric conditions and the position of the sun. Although data for this distribution is limited, a simple model may be inferred from the results of Yaroslavtzev [21]. Por-

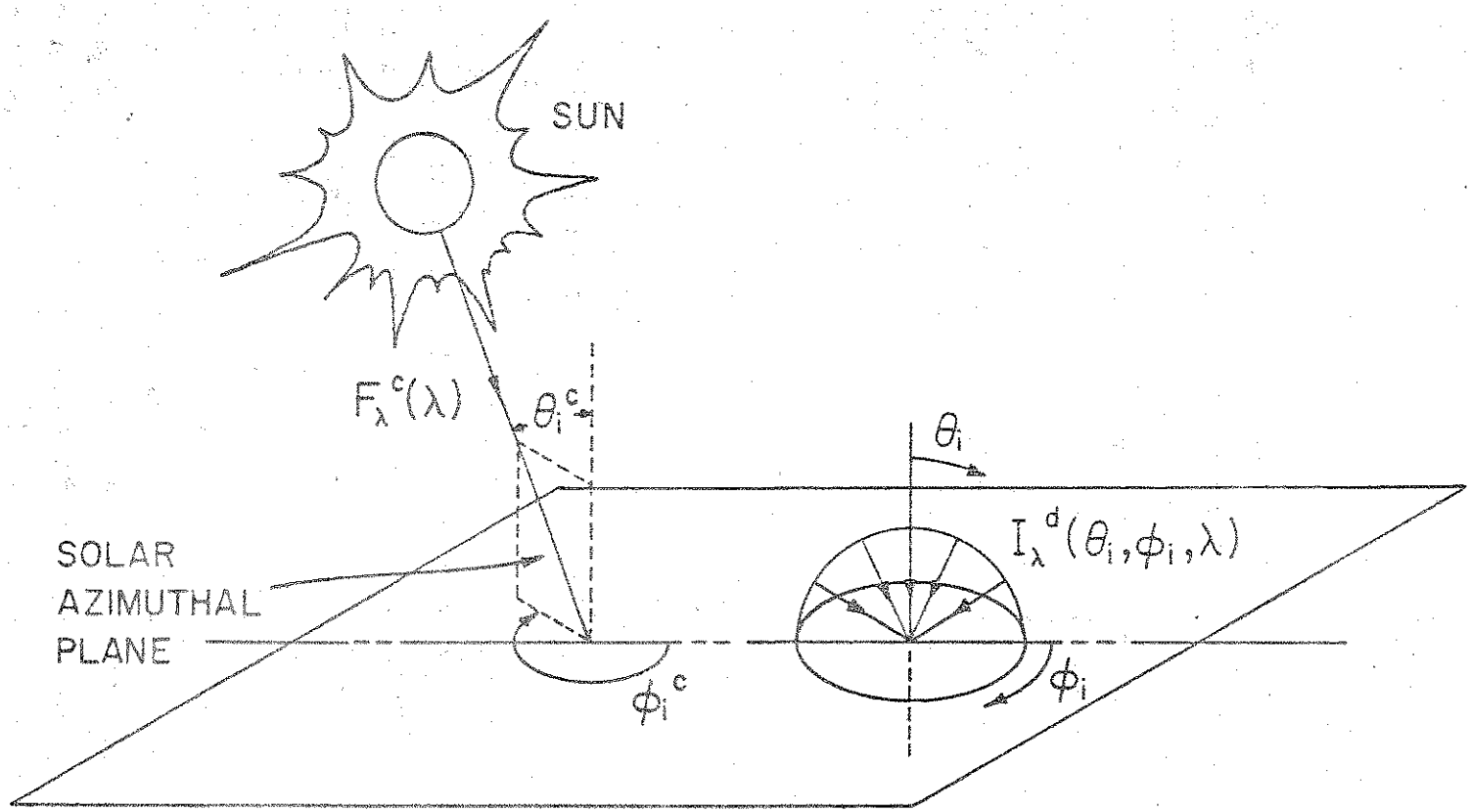

Figure 1. Collimated and diffuse components of the solar radiation incident on an algal pond.

tions of the data are plotted in Figs. 2 and 3. The quantity $\bar{I}_v^d$ is the radiance for the visible region of the spectrum normalized with respect to the visible radiance for $\theta_i = 0$, $\bar{I}_v^d(\theta_i,\phi_i) \equiv I_v^d(\theta_i,\phi_i)/I_v^d(0,\phi_i)$. The results in Fig. 2 pertain to a clear day with $\theta_i^c = 51°$, and those of Fig. 3 apply for complete cloud coverage with $\theta_i^c = 42°$. Two sets of data are presented on each figure, one for the solar azimuthal plane ($\phi_i = \phi_i^c$) and the other for a plane which is perpendicular to the solar azimuthal plane. For comparison $\cos\theta_i$ is also plotted. From the results it is evident that, for both clear and cloudy days, the diffuse radiance is sharply peaked in the direction of the collimated beam. That is, for $\theta_i \sim \theta_i^c$ in the solar azimuthal plane, there is a definite maximum in the diffuse radiance. However, if the shaded region under the maximum is ignored, the variation of the diffuse radiance with θ_i may be approximated by the cosine distribution. Moreover, in azimuthal planes well removed from the solar plane, there is no peak in the radiance and the entire distribution with θ_i is roughly approximated by the cosine function.

Collectively, the foregoing results suggest that, to a reasonable approximation, the diffuse radiance may be subdivided into two components. One component is assumed to be in the direction of θ_i^c and includes all of the diffuse radiation in the shaded region.[+] For the purpose of computing the radiation field within the algal pond, this component may therefore be combined with the collimated radiation. From the data of Yaroslavtzev [21], it was determined that approximately 20% of the total diffuse radiation was subject to this classification, in which case an effective collimated irradiance may be defined as

---

[+] It is implicit in this statement that, to determine the total amount of diffuse radiation in this category, an integration over the shaded regions in all of the azimuthal planes ($0 \leq \phi_i \leq 2\pi$) must be performed.

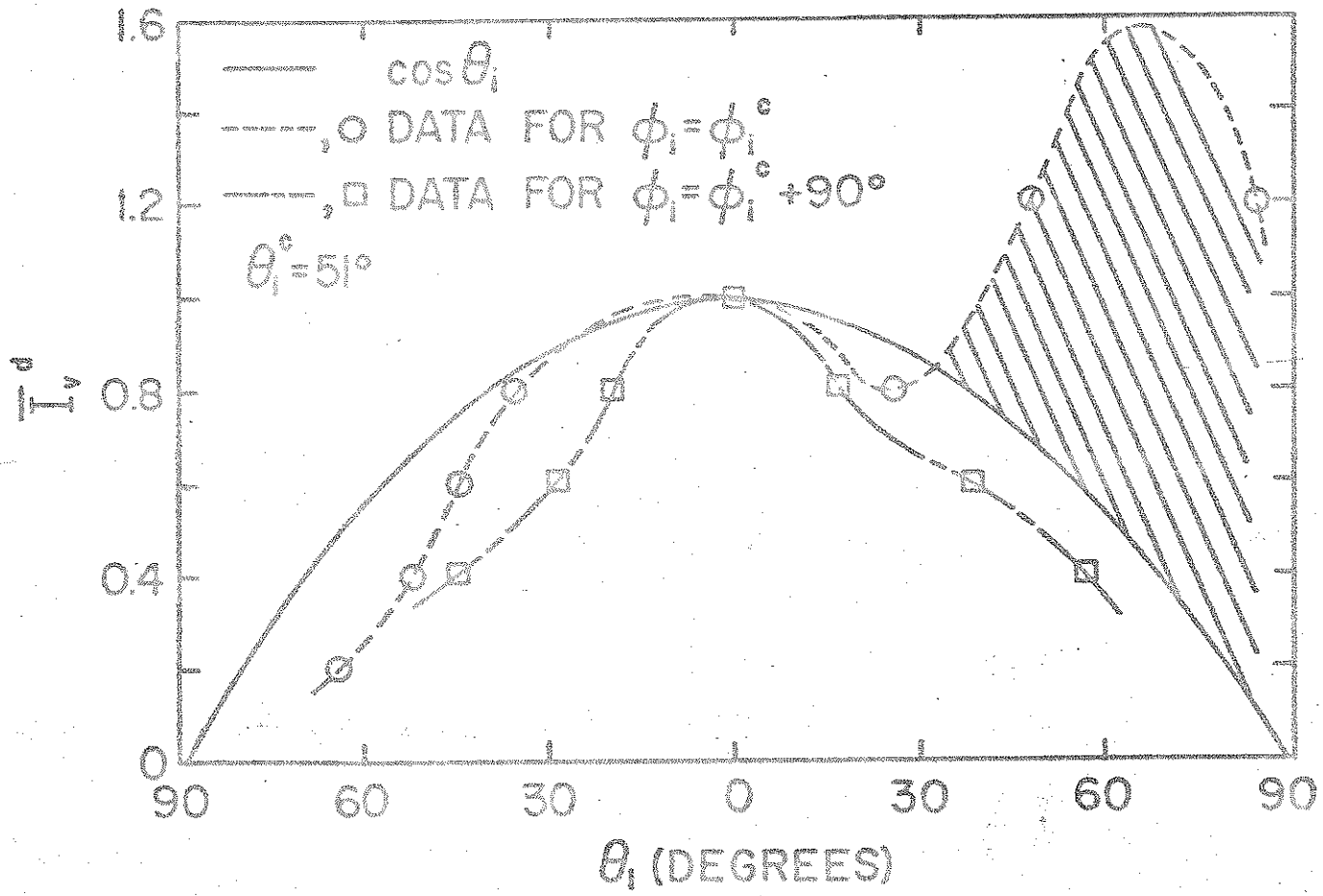

Figure 2. Normalized diffuse radiance for the visible spectrum as a function of incident angle for a clear day.

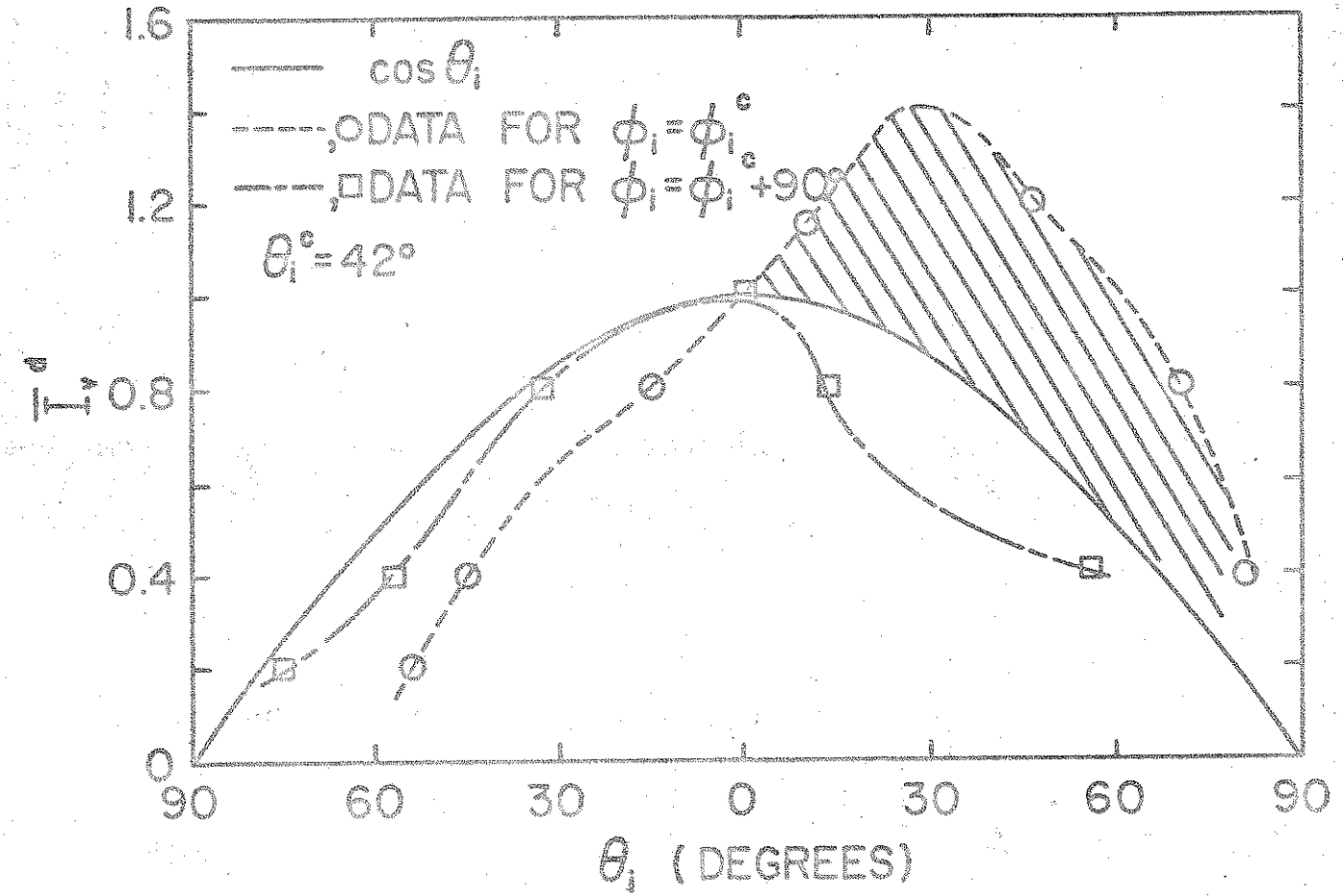

Figure 3. Normalized diffuse radiance for the visible spectrum as a function of incident angle for an overcast day.

$$F_\lambda^{C}(\lambda) = F_\lambda^{c}(\lambda) + 0.2F_\lambda^{d}(\lambda) \tag{17}$$

where F_λ^{d} is the monochromatic irradiance for the diffuse radiation.

The second, or residual, component of the diffuse radiation is assumed to vary with the cosine of θ_i and to be independent of ϕ_i. Accordingly, the angular distribution of this radiation may be represented as

$$I_\lambda^{D}(\theta_i,\phi_i,\lambda) = I_{\lambda,0}(\lambda)\cos\theta_i \tag{18}$$

where $I_{\lambda,0}$ corresponds to the radiance at $\theta_i = 0$. In general, irradiance may be related to radiance by an expression of the form [22]

$$F_\lambda(\lambda) = \int_0^{2\pi}\int_0^{\pi/2} I_\lambda(\theta_i,\phi_i,\lambda)\cos\theta_i\sin\theta_i d\theta_i d\phi_i \tag{19}$$

Hence substituting from (18) the remaining 80% of the diffuse radiation may be expressed as

$$0.8\ F_\lambda^{d}(\lambda) = 2\pi\ I_{\lambda,0}\int_0^{\pi/2}\cos^2\theta_i\sin\theta_i d\theta_i \tag{20}$$

Integrating, we obtain

$$0.8\ F_\lambda^{d}(\lambda) = (2\pi/3)I_{\lambda,0} \tag{21}$$

in which case $I_{\lambda,0}$ may be determined from knowledge of the diffuse irradiance F_λ^{d}.

It is also necessary to determine the spectral distribution of the incident solar radiation. For the direct component this distribution is a function of the sun's zenith angle θ_i^{c} and atmospheric conditions, such as cloud coverage and aerosol and water vapor concentrations [23,24].

To account for the effect of zenith angle, it is customary to work in terms of the relative air mass m, which is the ratio of the actual pathlength traversed by the collimated beam through the atmosphere to the pathlength associated with the zenith. The value of m may readily be determined as a function of θ_i^c [25]. The moisture content of the atmosphere, w, is measured in terms of the height of a vertical column of water which would form if all of the atmospheric vapor condensed. Procedures are available for determining w as a function of meteorological conditions [25].

Results for the spectral distribution of the collimated solar radiation at the earth's surface have been reported as a function of m and w [26]. Figs. 4 and 5 are based upon these results, with the spectral region having been subdivided into 10 nm bands. The ordinate axis provides the percent of the total collimated radiation which falls within the 10 nm band. Results such as these, together with knowledge of the total collimated irradiance F^c may be used to obtain the desired spectral distribution. Due to the variability of conditions and the absence of sufficient data, it is impractical at this time to attempt to account for the effects of cloud coverage and extraneous molecular and particulate constituents on the spectral distribution.

Because radiation scattering by atmospheric gases increases with decreasing wavelength, the spectrum of the diffuse radiation is shifted to shorter wavelengths compared to that of the collimated radiation. The spectral distribution of the diffuse radiation depends upon the direction of the collimated beam, the polar and azimuthal angles of the diffuse radiation, cloud coverage and atmospheric conditions [23,24]. However, since little data is available concerning the extent to which the diffuse spectrum changes with these variables, it was

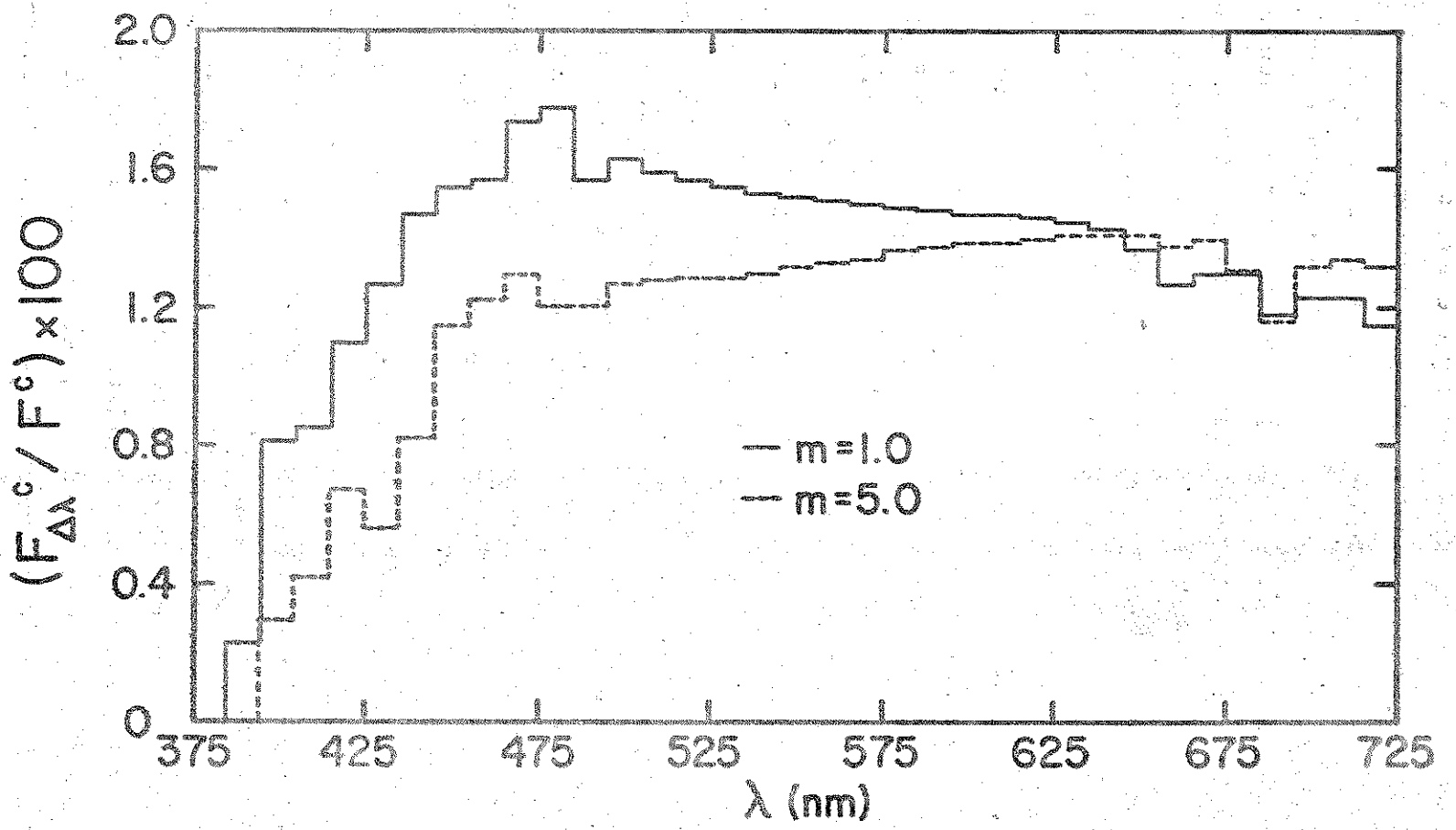

Figure 4. Spectral distribution of the collimated solar radiation ($w=5 \times 10^{-2}$ cm).

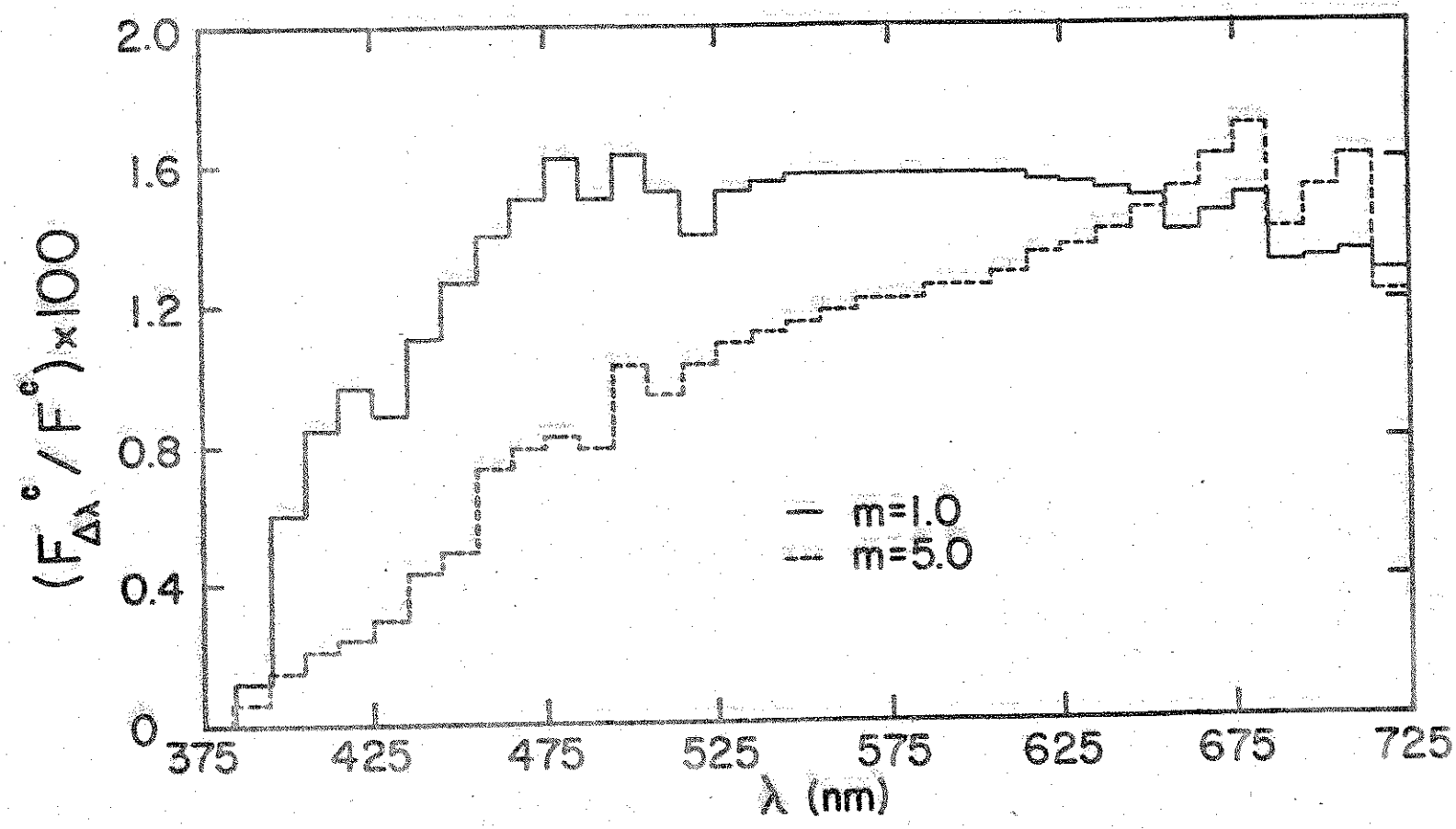

Figure 5. Spectral distribution of the collimated solar radiation (w=1.37 cm).

necessary to work with a single distribution which is representative of actual conditions. The spectral distribution of Fig. 6 was constructed from existing results [24] and was used in the calculations of this study.

To quantify the spectral distribution of both solar radiation components and the angular distribution of the diffuse component incident on the pond, it only remains to determine the total collimated and diffuse irradiances, F^c and F^d, where

$$F^c \equiv \int_o^\infty F_\lambda{}^c d\lambda \tag{22}$$

$$F^d \equiv \int_o^\infty F_\lambda{}^d d\lambda \tag{23}$$

In most instances one is interested in determining diurnal and seasonal growth conditions for a particular geographical location. Hence for a prescribed location it is necessary to know the variation of F^c and F^d with time. Although several procedures are available for determining these quantities, the method chosen for this study is one which incorporates available meteorological data [27]. The procedure was first suggested by Kimball [28] and described in detail in a more recent publication [25]. The collimated and diffuse irradiances on a horizontal surface at ground level for a clear day are expressed as

$$F_c{}^c = (a''-d)F_o \tag{24}$$

$$F_c{}^d = [0.5(1-a')+d]F_o \tag{25}$$

The quantity F_o is the extraterrestrial solar irradiance on a horizontal surface, and its diurnal and seasonal variation for a prescribed geographical location may be accurately determined from standard procedures [20,25].

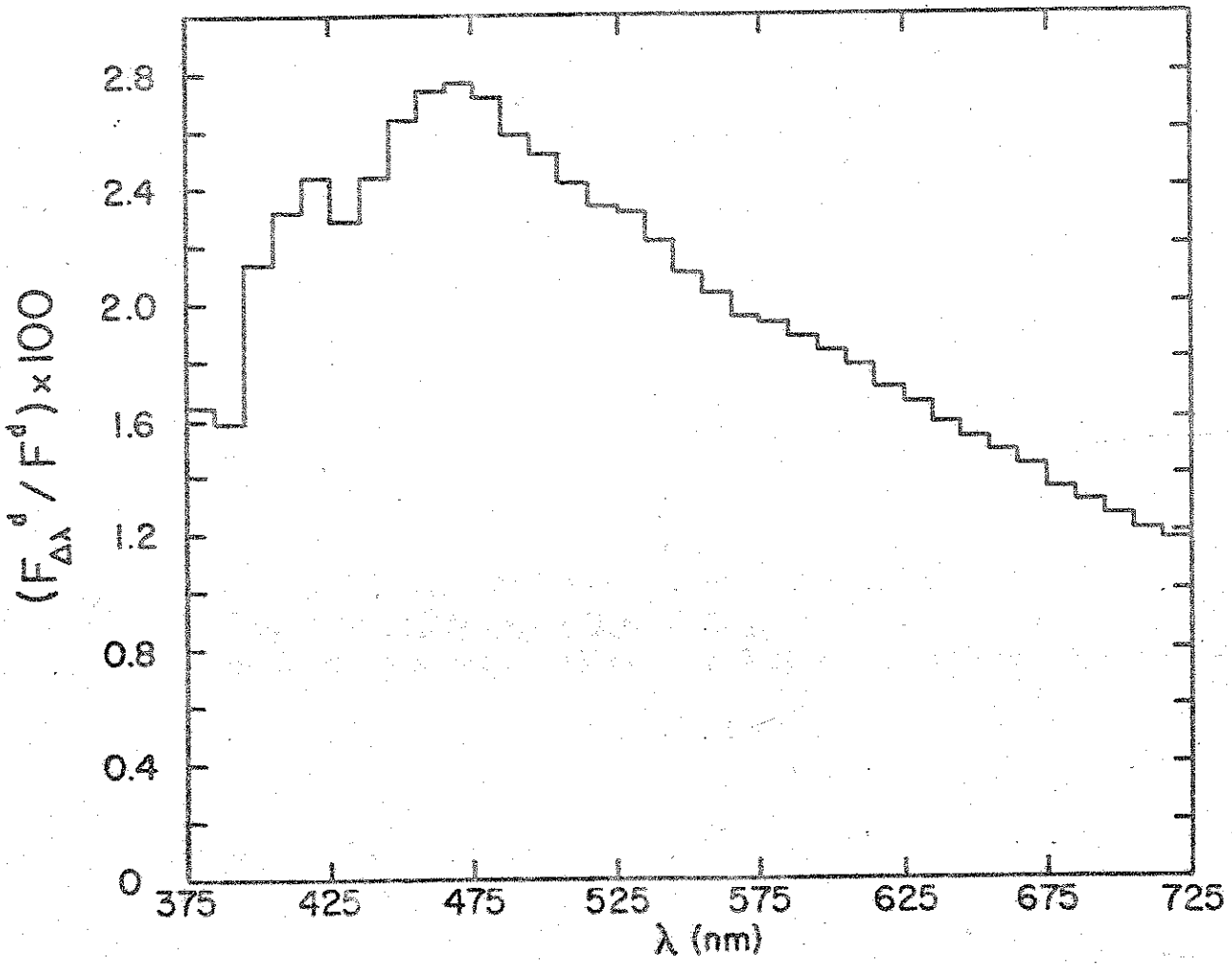

Figure 6. Spectral distribution of the diffuse solar radiation.

The atmospheric transmission coefficients a" and a' are functions of the relative air mass m and the atmospheric moisture content w and may be computed from the following correlations [25]

$$a"=\exp\{m[-(0.465+0.13w)][0.179+0.421\exp(-0.721m)]\} \quad (26)$$

$$a'=\exp\{m[-(0.465+0.13w)][0.129+0.171\exp(-0.880m)]\} \quad (27)$$

The dust depletion coefficient d may range from 0.01 to 0.13 [29], depending upon air mass, time of year and the extent of agricultural and industrial activity within the region of interest. A representative value of 0.06 was used for the calculations of this study.

The incident solar radiation is further attenuated by the presence of cloud cover, and several empirical relations have been proposed for relating the solar irradiance under cloudy skies to that under clear skies. The relations are of the general form

$$F \equiv F^c + F^d = f(C)\cdot F_c = f(C)\cdot (F_c{}^c + F_c{}^d) \quad (28)$$

where C is the fraction of the sky which is covered by clouds. It is expressed in tenths and may range from 0 (clear skies) to 10 (completely overcast). Alternatively, the effects of cloud coverage may be treated in terms of the percent sunshine factor S, which is defined as the actual solar radiation incident on a horizontal surface for a given day relative to the amount of radiation which would have been incident on the surface had clear skies prevailed throughout the day. Accordingly,

$$S \equiv \frac{\int_0^{24} F\, dt}{\int_0^{24} F_c dt} \quad (29)$$

The value of S is 100 if clear skies prevail throughout the 24 hour period and approaches 0 for completely cloudy skies. Although values of both C and S are normally provided with weather data, it was decided to use the sunshine factor for the calculations of this study, since it provides a more accurate measure of the actual insolation. When using this quantity for calculations over a diurnal period, it is assumed that S is constant throughout the day and equivalent to the value prescribed for the entire day.

Unfortunately, most of the existing efforts to treat the effects of cloud coverage are based upon the total solar radiation and are therefore insufficient for the purposes of this study. In any case, to separately account for the effects of cloud cover on the collimated and the diffuse components of the solar radiation, it is necessary to make certain assumptions. First it is assumed that solar radiation absorption by the clouds is negligible and that all of the collimated radiation which is incident on a cloud is converted to diffuse radiation. One implication of this assumption is that the collimated irradiance on a cloudy day may be approximated as

$$F^C = (1 - \frac{C}{10})F_c{}^C \tag{30}$$

If it is further assumed that C and S are related by an expression of the form,

$$(1 - \frac{C}{10}) = \frac{S}{100} \tag{31}$$

equation (30) may be expressed as

$$F^C = (\frac{S}{100})F_c{}^C \tag{32}$$

If it is also assumed that, irrespective of the nature of the incident radiation, the albedo of the clouds is 0.5, the

diffuse irradiance may be approximated as

$$F^d = (1 - \frac{C}{10})F_c^d + 0.5(F_c^c + F_c^d)\frac{C}{10} \qquad (33)$$

or, in terms of the percent sunshine,

$$F^d = (\frac{S}{100})F_c^d + 0.5(F_c^c + F_c^d)(1 - \frac{S}{100}) \qquad (34)$$

The use of an albedo of 0.5 for clouds is justified on the basis of measurements [24].

Although approximate in nature, it is felt that the foregoing model may be used to obtain a reasonable estimate of the diffuse and direct components of the solar irradiance on an algal pond. The percent sunshine data required for the calculations may be obtained from actual weather data compiled by the National Climatic Center [27]. The specific data used in this study is for Indianapolis, Indiana during the year 1974.

In summary, the directional distribution of the diffuse radiation is obtained from (18), where the normal radiance $I_{\lambda,0}$ is determined from (21). The spectral distributions, F_λ^c and F_λ^d, are obtained from plots such as those in Figs. 4 through 6, where F^c and F^d are determined from (32) and (34). The effective collimated radiation may then be determined from (17).

3.2 The Air-Water Interface

The next step in the radiation analysis involves determining the reflection and refraction of the incident solar radiation at the air-water interface (Fig. 7). Assuming this interface to be a smooth, specularly reflecting surface and neglecting polarization effects, the surface reflectivity may be obtained from Fresnel's equation [30]

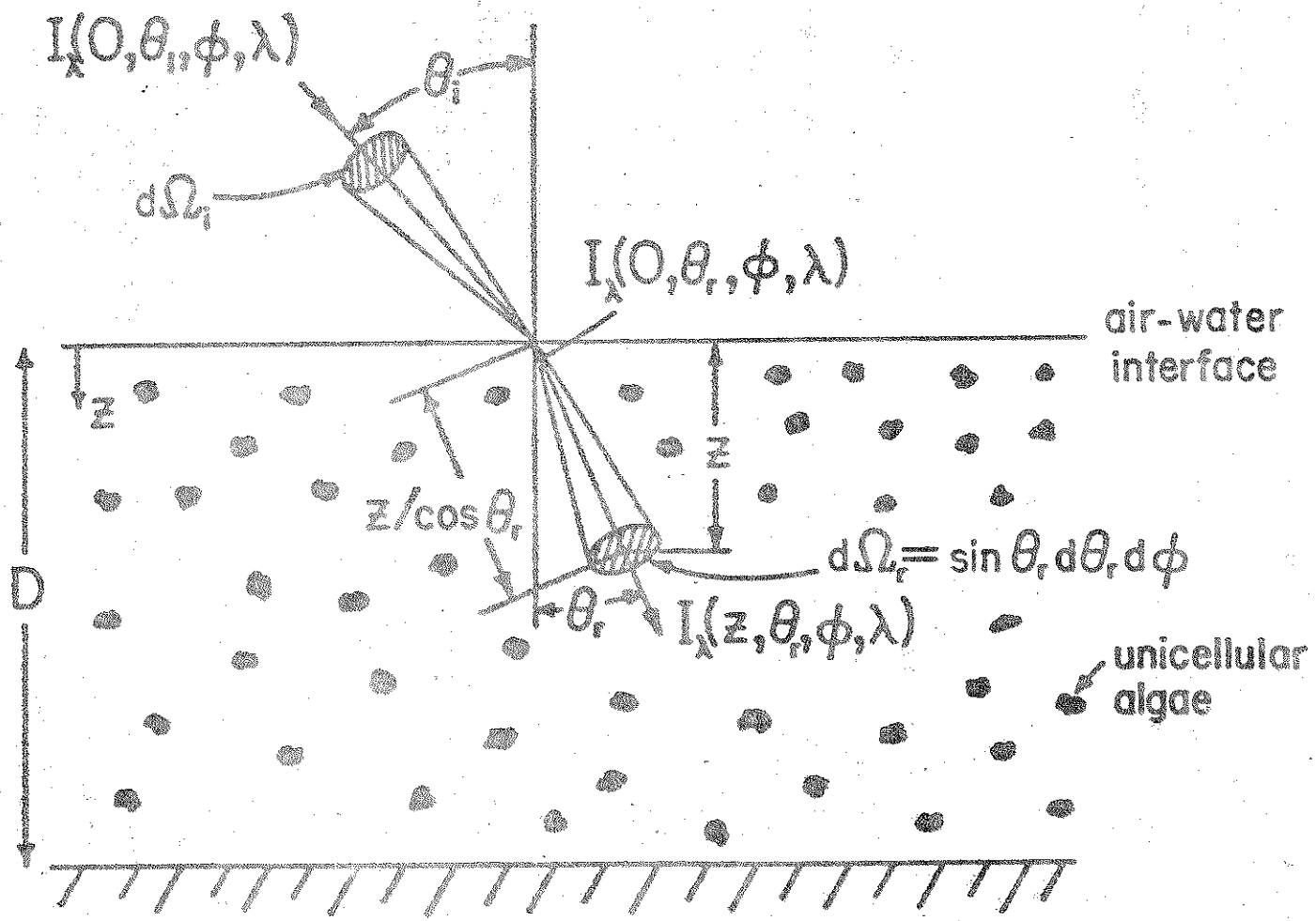

Figure 7. Refraction of incident solar radiation at the air-water interface.

$$\rho(\theta_i) = \frac{1}{2}\left[\frac{\sin^2(\theta_i-\theta_r)}{\sin^2(\theta_i+\theta_r)} + \frac{\tan^2(\theta_i-\theta_r)}{\tan^2(\theta_i+\theta_r)}\right] \tag{35}$$

where θ_i determines the direction of the incident radiation relative to the zenith and θ_r determines the direction of the refracted radiation relative to the nadir. The angle of refraction may be related to the incident angle through Snell's law

$$\theta_r = \sin^{-1}\left(\frac{\sin\theta_i}{n}\right) \tag{36}$$

where n is the refractive index for radiation propagating from air into water (n~1.33). According to (36) the critical angle of refraction, corresponding to θ_i=90°, is θ_r=48.75°. The transmissivity of the air-water interface is simply

$$\tau(\theta_i) = 1 - \rho(\theta_i) \tag{37}$$

From the foregoing results it is a simple matter to obtain the irradiance $F_\lambda^C(0,\lambda)$ of the effective collimated radiation in the water just below the pond surface. In particular

$$F_\lambda^C(0,\lambda) = \tau(\theta_i^C)F_\lambda^C(\lambda) \tag{38}$$

where F_λ^C, the irradiance in the air just above the surface, may be determined from (17). Below the surface the collimated radiation propagates in the direction θ_r of the refracted radiation. To obtain the radiance $I_\lambda^D(0,\theta_r,\phi,\lambda)$ of the diffuse radiation just below the pond surface, it is necessary to account for both the surface reflection and the enhancement of this radiation due to refraction. That

is, the radiation incident over $0 \leq \theta_i \leq 90°$ is refracted into a cone of $0 \leq \theta_r \leq 48.75°$, and the resulting enhancement of the refracted radiance is known to be of the form [30]

$$I^D(\theta_r) = n^2 \, I^D(\theta_i) \tag{39}$$

Accordingly, the radiance of the residual diffuse radiation just below the pond surface is

$$I_\lambda{}^D(0,\theta_r,\phi,\lambda) = n^2 \, \tau(\theta_i) I_\lambda{}^D(\theta_i,\phi,\lambda) \tag{40}$$

where $I_\lambda{}^D(\theta_i,\phi,\lambda)$, the radiance in the air just above the surface, is determined from (18).

3.3 Radiation Transfer Within the Pond

The results of the foregoing sections may be used to determine the magnitude and the spectral and angular distributions of the refracted solar radiation. To determine the extent to which this radiation is absorbed by the algae, it is now necessary to determine the radiation field within the pond.

An algal pond is an absorbing-scattering medium comprised of particles suspended in a liquid substrate (Fig. 7). In the most general case scattering may be effected by bacterial cells and nutrient particles, as well as by algal cells, and absorption may be effected by both the substrate and the particulates. In this study, however, absorption and scattering will be assumed to be due exclusively to the algal cells. This assumption is necessitated by the fact that the required optical property data is only available for algal suspensions which are cultured on synthetic nutrient media. There is presently no optical property data for symbiotic cultures in which significant absorption and scattering may be due to several constituents.

Nevertheless, the assumption should provide a reasonable approximation to visible radiation transfer in dense algal cultures. Moreover, as optical property data becomes available for symbiotic cultures, refinements to the calculations may readily be made.

The radiation field in the suspension may be obtained by solving the quasi-steady-state equation of transfer. For negligible polarization in a planar, scattering-absorbing medium, the equation is of the form [22]

$$\cos\theta_r \frac{dI_\lambda(z,\Omega_r,\lambda)}{dz} = -\beta_\lambda I_\lambda(z,\Omega_r,\lambda) + \frac{\sigma_\lambda}{4\pi}\int_0^{2\pi}\int_0^{\pi} I_\lambda(z,\Omega',\lambda)P_\lambda(\Omega'\rightarrow\Omega_r)d\Omega' \qquad (41)$$

where $I_\lambda(z,\Omega_r,\lambda)$ is the monochromatic radiance in the culture. The optical properties of algae required for the solution of (41) include the extinction coefficient β_λ, the scattering coefficient σ_λ and the normalized phase function P_λ. The extinction coefficient is comprised of absorbing and scattering components ($\beta_\lambda=\alpha_\lambda+\sigma_\lambda$). The above expression describes the change with respect to the z coordinate of the radiance of a beam of monochromatic radiation propagating in the direction of the solid angle Ω_r. The radiance will be diminished due to scattering and absorption by algal cells, and it may be increased due to radiation scattering from other directions Ω' into Ω_r.

There exist numerous schemes for solving the equation of transfer in scattering-absorbing media, with the complexity depending upon the degree to which one wishes to determine the directional characteristics of the radiation field [22,31]. In a recent study [32] four such methods, which vary widely in their level of sophistication, were used to predict radiation absorption and scattering by solids suspended in water. The methods ranged from the highly simplistic one-flux (Beer-Lambert) model to the

method of discrete ordinates, which is capable of providing a high-order estimate of the radiation field. Through variation of the number of ordinates, it can be used to predict the radiation field to whatever detail desired. The other two methods are of intermediate order and involve the use of two-flux and six-flux approximations.

Calculations based upon the aforementioned models were performed using optical property data for C. pyrenoidosa [32]. An important feature of this data is the fact that the phase function is very sharply peaked in the forward direction. A major implication of this result is that a beam of radiation would have to experience numerous scatterings before it became appreciably diverged from the original direction of propagation. For this reason the comparative calculations [32] revealed that, irrespective of the directional distribution and the relative contributions of the direct and diffuse components of the incident radiation, the Beer-Lambert law provided a good approximation to the radiation field in an algal suspension. The methods were compared on the basis of the amount of radiation absorbed per unit volume at different depths in the culture, and the Beer-Lambert results were found to be in good agreement with those obtained from the discrete ordinate and six-flux methods. Since the suitability of the Beer-Lambert law for predicting radiation attenuation in algal cultures has also been confirmed experimentally [11,12], the method was selected for use in the calculations of the present study.

If multiple scattering effects are neglected, equation (41) reduces to

$$\cos\theta_r \frac{dI_\lambda(z,\Omega_r,\lambda)}{dz} = -\beta_\lambda I_\lambda(z,\Omega_r,\lambda) \qquad (42)$$

Performing the integration over z for a prescribed beam direction we then obtain

$$I_\lambda(z,\Omega_r,\lambda) = I_\lambda(0,\Omega_r,\lambda)\ \exp(-\beta_\lambda \frac{z}{\cos\theta_r}) \tag{43}$$

where $I_\lambda(0,\Omega_r,\lambda)$ is the radiance of the refracted radiation at z=0. However, for collimated radiation propagating in the direction θ_r, (43) can also be used to determine the variation of the irradiance with depth. That is,

$$F_\lambda^C(z,\lambda) = F_\lambda^C(0,\lambda)\ \exp(-\beta_\lambda \frac{z}{\cos\theta_r}) \tag{44}$$

where $F_\lambda^C(0,\lambda)$, the irradiance of the collimated radiation just below the pond surface, is obtained from (38). The total irradiance in the visible region is then given by

$$F_V^C(z) = \int_{380}^{720} F_\lambda^C(0,\lambda)\ \exp(-\beta_\lambda \frac{z}{\cos\theta_r})d\lambda \tag{45}$$

The irradiance associated with the diffuse radiation can be determined by substituting (43) into (19). Hence

$$F_\lambda^D(z,\lambda) = \int_0^{2\pi}\int_0^{48.75^\circ} I_\lambda^D(0,\Omega_r,\lambda)\exp(-\beta_\lambda \frac{z}{\cos\theta_r})\cos\theta_r\ \sin\theta_r\ d\theta_r\ d\phi \tag{46}$$

or, for axially symmetric conditions,

$$F_\lambda^D(z,\lambda) = 2\pi \int_0^{48.75^\circ} I_\lambda^D(0,\Omega_r,\lambda)\exp(-\beta_\lambda\frac{z}{\cos\theta_r})\cos\theta_r\ \sin\theta_r\ d\theta_r \tag{47}$$

The angle θ_r=48.75° is the critical angle which forms the cone into which all of the incident radiation must be refracted, and $I_\lambda^D(0,\Omega_r,\lambda)$, the radiance of the refracted radiation at z=0, is determined from (40). The total diffuse irradiance in the visible region of the spectrum is then

$$F_v^D(z) = 2\pi \int_{380}^{720} \int_{0}^{48.75^\circ} I_\lambda^D(0,\Omega_r,\lambda)\exp(-\beta_\lambda \frac{z}{\cos\theta_r})\cos\theta_r \sin\theta_r d\theta_r d\lambda \tag{48}$$

The foregoing results may be used to determine the local rate of solar radiation absorption by the algae. In particular the monochromatic volumetric absorption (einstein·m^{-3}·hr^{-1}·nm^{-1}) is related to the irradiance by an expression of the form

$$H_\lambda(z,\lambda) = \frac{\partial F_\lambda(z,\lambda)}{\partial z} \tag{49}$$

where

$$F_\lambda(z,\lambda) \equiv F_\lambda^C + F_\lambda^D \tag{50}$$

It is tacitly assumed that scattering is negligible and that all of the radiation absorption is due to the algae, an assumption which is reasonable for dense cultures.

To calculate the radiation field in the culture, the extinction coefficient $\beta_\lambda(\lambda)$ must be known. For this study the results obtained by Dabes [11] for C. pyrenoidosa will be used. The variation of the extinction coefficient with λ is shown in Fig. 8. However it should be noted that the results are in units of m^2·mg(chlorophyll)$^{-1}$. The relation between the extinction coefficient β_λ' in these units to the extinction coefficient β_λ in m^{-1} is

$$\beta_\lambda'[m^2 \cdot mg(\text{chlorophyll})^{-1}] = \frac{\beta_\lambda(m^{-1})}{C_a r_c} \tag{51}$$

where C_a is the algal mass density in mg(dry mass algae)·m^{-3} and r_c is the mass fraction of chlorophyll in the algae in units of mg(dry mass chlorophyll)·mg(dry mass algae)$^{-1}$.

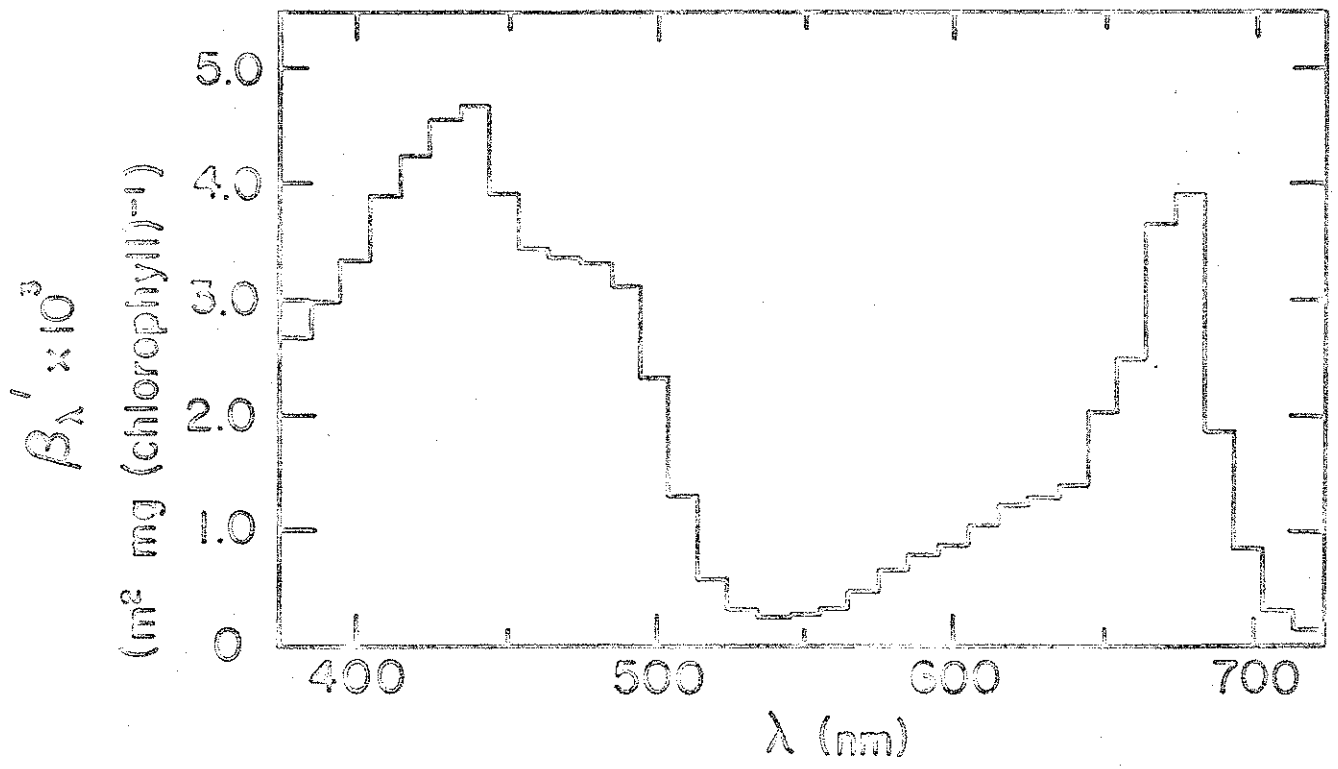

Figure 8. Extinction coefficient $\beta_\lambda'(\lambda)$ used for the calculations of this study. From Dabes et al. [11].

Both C_a and r_c are readily measured properties of an algal culture, and it is convenient to combine them with the depth z to form an integrated chlorophyll concentration of the form

$$C_c \equiv C_a \, r_c \, z \tag{52}$$

The quantity C_c, which has units of mg(chlorophyll)$\cdot m^{-2}$, is the total mass of chlorophyll which occupies a volume of unit area and of length z. Substituting equations (51) and (52) into (44), we may then write for the collimated monochromatic irradiance at z

$$F_\lambda^C(z,\lambda) = F_\lambda^C(0,\lambda)\exp\left(-\frac{\beta_\lambda' C_c}{\cos\theta_r}\right) \tag{53}$$

Similarly, from (47) the diffuse irradiance may be expressed as

$$F_\lambda^D(z,\lambda) = 2\pi \int_0^{48.75°} I_\lambda^D(0,\Omega_r,\lambda)\exp\left(-\frac{\beta_\lambda' C_c}{\cos\theta_r}\right)\cos\theta_r \sin\theta_r \, d\theta_r \tag{54}$$

With F_λ^C and F_λ^D given by (53) and (54), the volumetric absorption may also be expressed as

$$H_\lambda'(C_c,\lambda) = \frac{\partial F_\lambda(C_c,\lambda)}{\partial C_c} \tag{55}$$

where H_λ' has the units of einstein$\cdot$mg(chlorophyll)$^{-1}\cdot$ $hr^{-1}\cdot nm^{-1}$ and

$$H_\lambda'(C_c,\lambda) = \frac{H_\lambda(z,\lambda)}{C_a \, r_c} \tag{56}$$

From equation (4) the light dependent kinetic parameter R_A may now be expressed as

$$R_A = \int_{380}^{720} \phi_\lambda(\lambda) H_\lambda'(C_c,\lambda) \, d\lambda \tag{57}$$

or, with the quantum yield for oxygen evolution assumed to be a constant, $\phi_\lambda = \phi = 0.1138$,

$$R_A = 0.1138 \int_{380}^{720} H_\lambda'(C_c, \lambda) d\lambda \qquad (58)$$

where H_λ' is obtained from (50), (53), (54), and (55).

CHAPTER 4 RESULTS

4.1 Computational Procedures

The foregoing model may be used to compute algal growth under field conditions, and a computer program has been developed for this purpose. The required input data includes

(i) the magnitudes of the incident direct and diffuse solar radiation (obtained from (24), (25), (32), and (34) along with available meteorological data [27]),

(ii) the zenith angle θ_i^c of the incident collimated radiation and the atmospheric mass m and moisture content w (determined from standard procedures [25]),

(iii) the spectral distribution of the collimated radiation (obtained from Figs. 4 and 5, using linear interpolation with m and w as parameters) and the spectral distribution of the diffuse radiation (Fig. 6), and

(iv) the extinction coefficient (Fig. 8).

Calculations of the radiation field are complicated by the need to perform both spectral and directional integrations. From equation (53) the magnitude of the monochromatic collimated radiation is calculated as a function of the integrated chlorophyll concentration C_c for each 10 nm band between 380 and 720 nm. Moreover, the diffuse radiation is subdivided to angular intervals of $\Delta\theta_r=3.25°$, as well as into spectral bands of 10 nm. A modified version of (54), for which the integration is restricted to the angular interval $\Delta\theta_r$, may then be applied to determine the diffuse radiation as a function of C_c. For a particular value of C_c the monochromatic diffuse irradiance may then be determined by summing over the contributions from each of the angular intervals. At each C_c of interest the collimated and diffuse monochromatic irradiances may then be added, and (55) may then be applied to determine the absorbed radiation. The results for the different spectral bands may then be substituted into (57) and the kinetic

model used to determine oxygen and algal biomass production.

4.2 The Radiation Field

All calculations of this study were performed for a pond which is presumed to be located in Indianapolis, Indiana (Latitude 39° 44' N, Longitude 86° 17' W, Elevation 241 m). The solar irradiance may be determined as a function of time of day and year, and diurnal variations for four representative days are shown in Figures 9 to 12. Although the results pertain to the entire spectrum ($0 \leq \lambda \leq \infty$), multiplication by a factor of 0.45 will provide the approximate contribution of the PhAR [35]. The results have been delineated in terms of the total, collimated and diffuse irradiances for 100% sunshine and the total irradiance for 0% sunshine (complete cloud coverage). For S=0 the total irradiance is, of course, comprised exclusively of the diffuse contribution. The results provide an indication of the extremes which may be expected due to seasonal and cloud coverage effects, with maximum insolation corresponding to 100% sunshine in June and minimum insolation corresponding to 0% sunshine in December. Intermediate results are presented for the months of March and September. However, since conditions are nearly equivalent for the two months, subsequent results will be presented only for March.

The nature of the radiation field in an algal culture may be inferred from the results in Figures 13 to 16. Figures 13 and 14 present the irradiance for the visible region of the spectrum ($380 \leq \lambda \leq 720$) at solar noon as a function of the integrated chlorophyll concentration, which is defined by (52). Figures 15 and 16 present the corresponding results for the local rate of radiation absorption per mg (chlorophyll). Use of the integrated chlorophyll concentration as an independent variable renders the results more general, since they may then be used for any value of C_a, r_c or z.

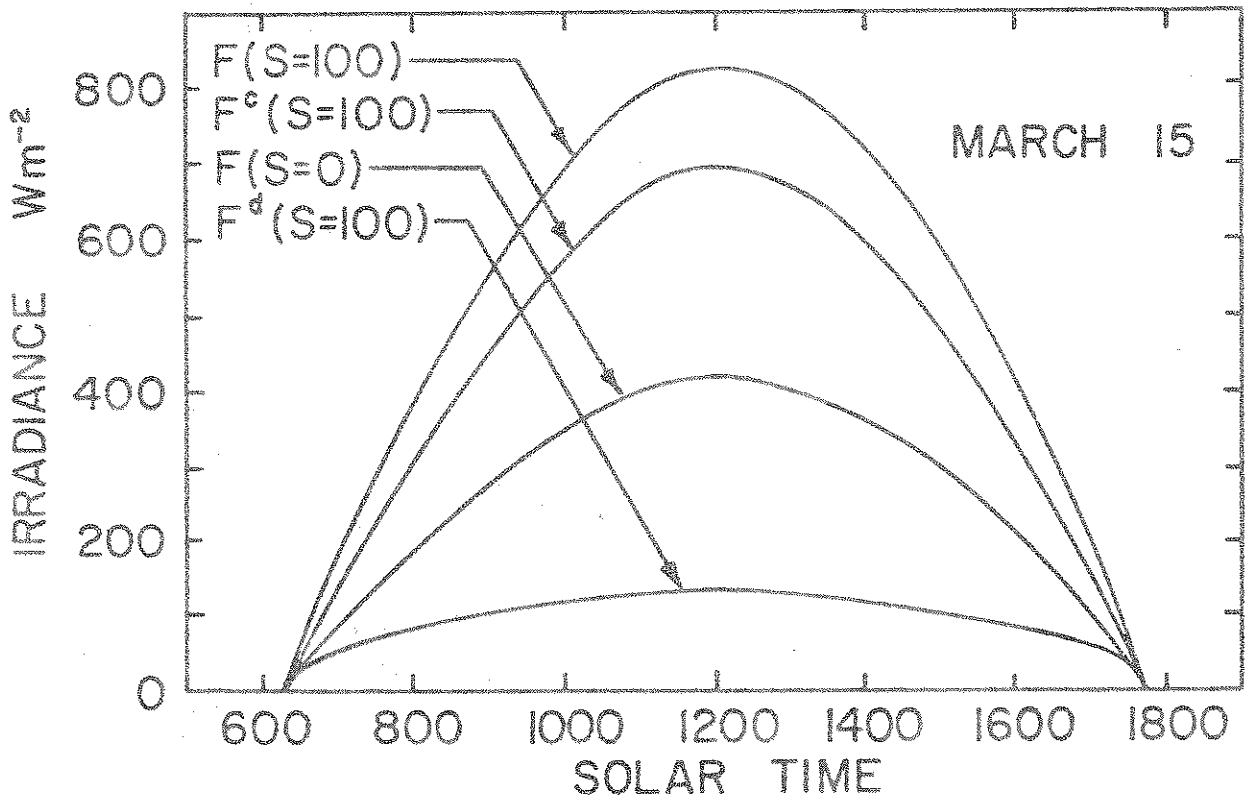

Figure 9. Hourly variation in the solar irradiance for Indianapolis, Indiana on March 15.

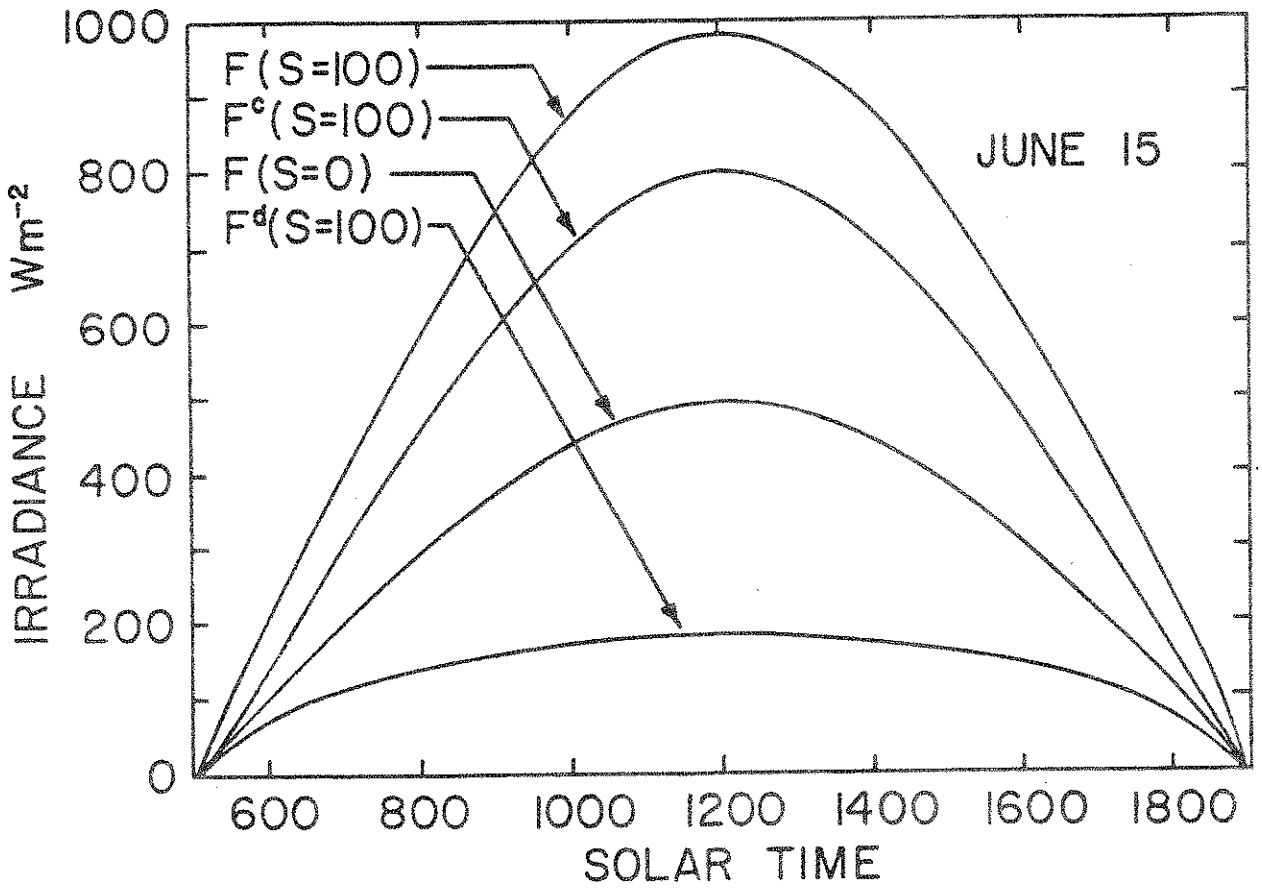

Figure 10. Hourly variation in the solar irradiance for Indianapolis, Indiana on June 15.

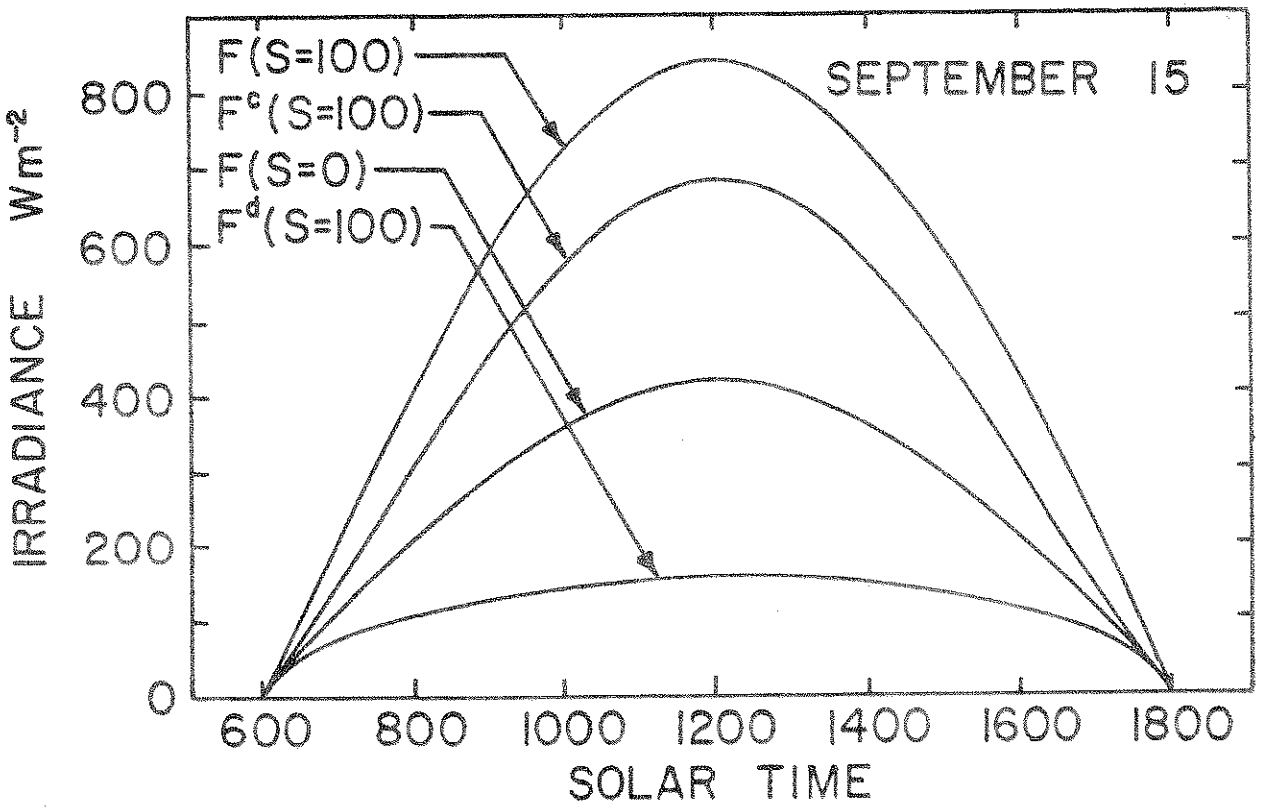

Figure 11. Hourly variation in the solar irradiance for Indianapolis, Indiana on September 15.

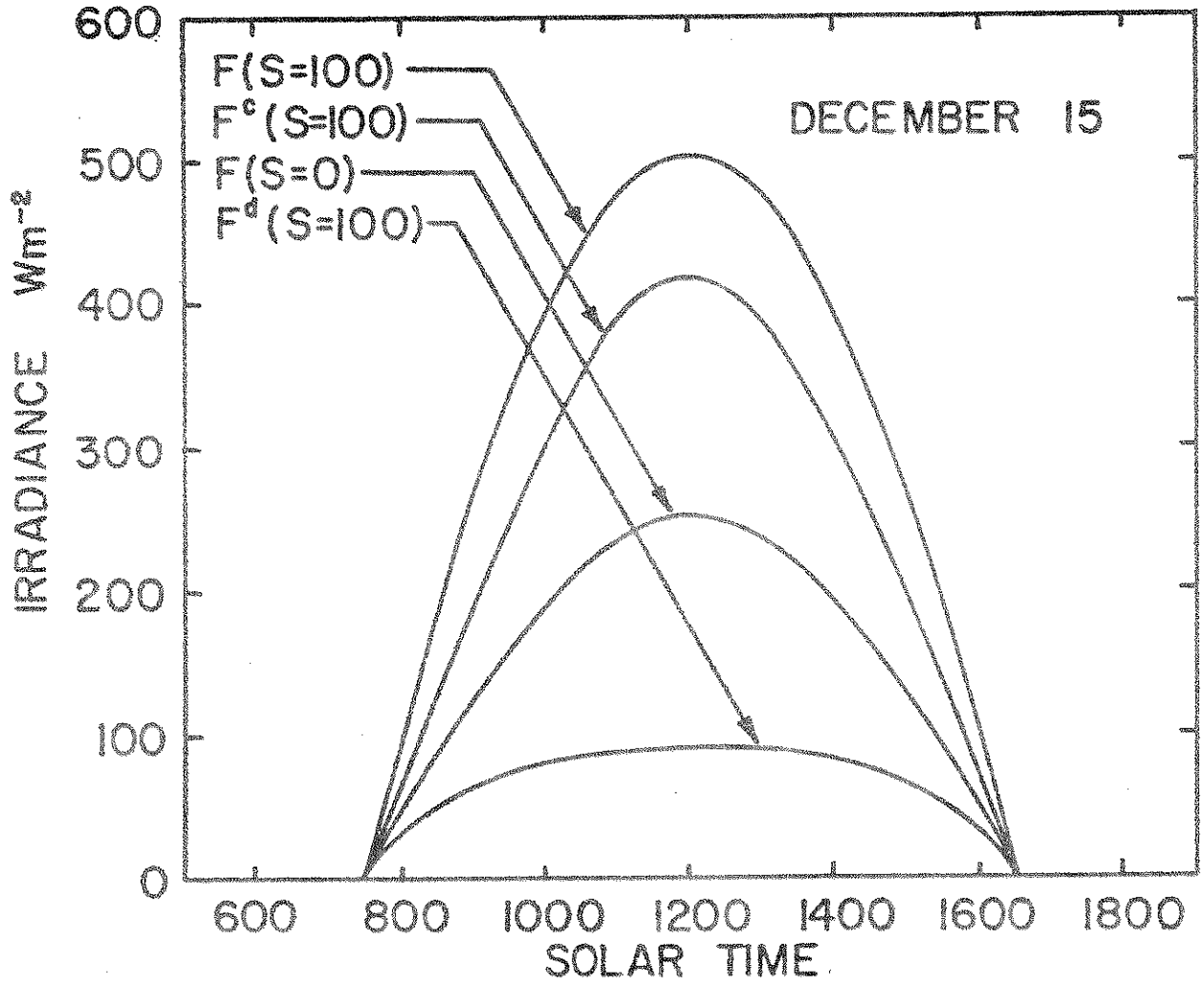

Figure 12. Hourly variation in the solar irradiance for Indianapolis, Indiana on December 15.

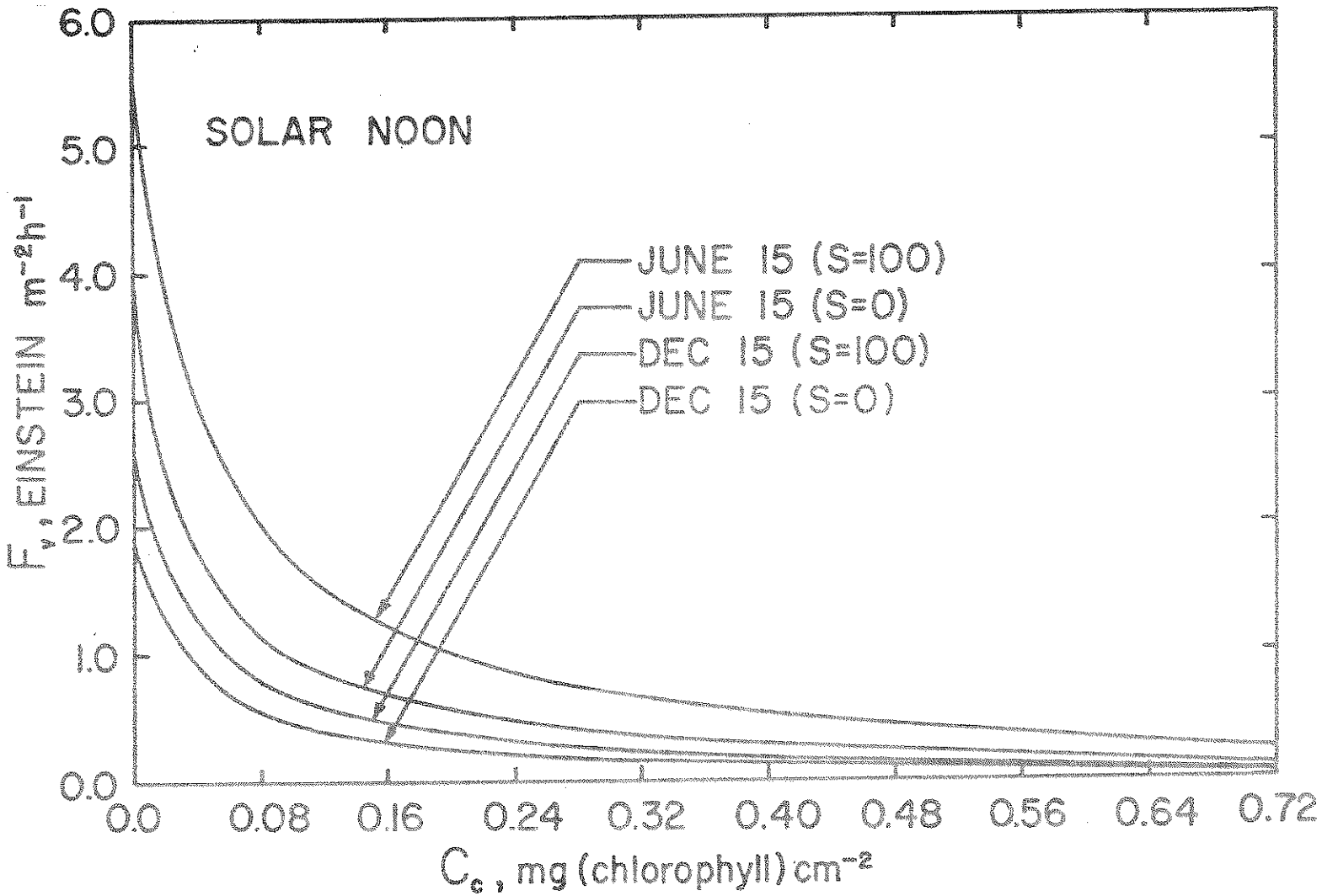

Figure 13. Solar irradiance for the visible region of the spectrum as a function of integrated chlorophyll concentration at solar noon on June 15 and December 15.

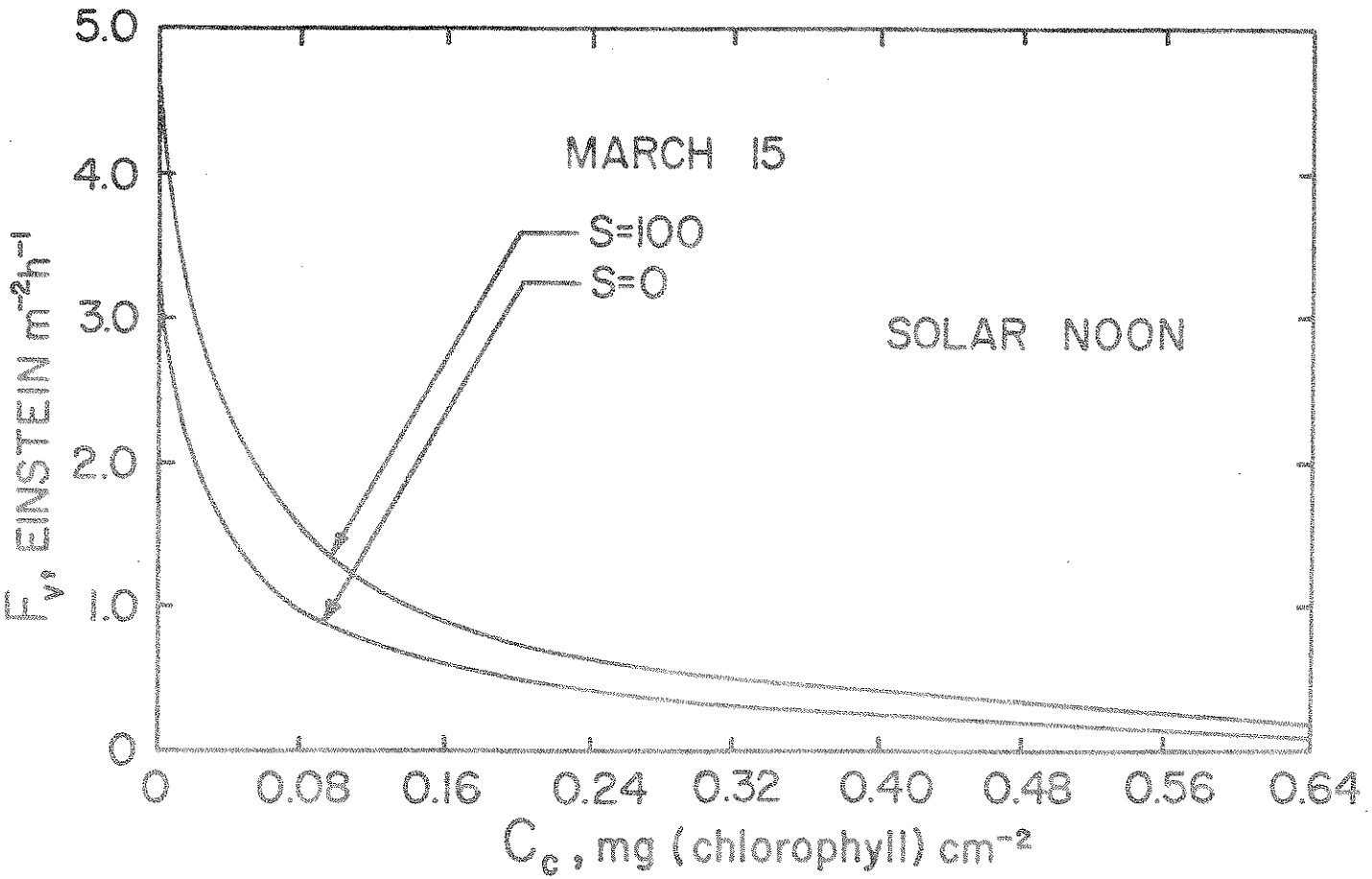

Figure 14. Solar irradiance for the visible region of the spectrum as a function of integrated chlorophyll concentration at solar noon on March 15.

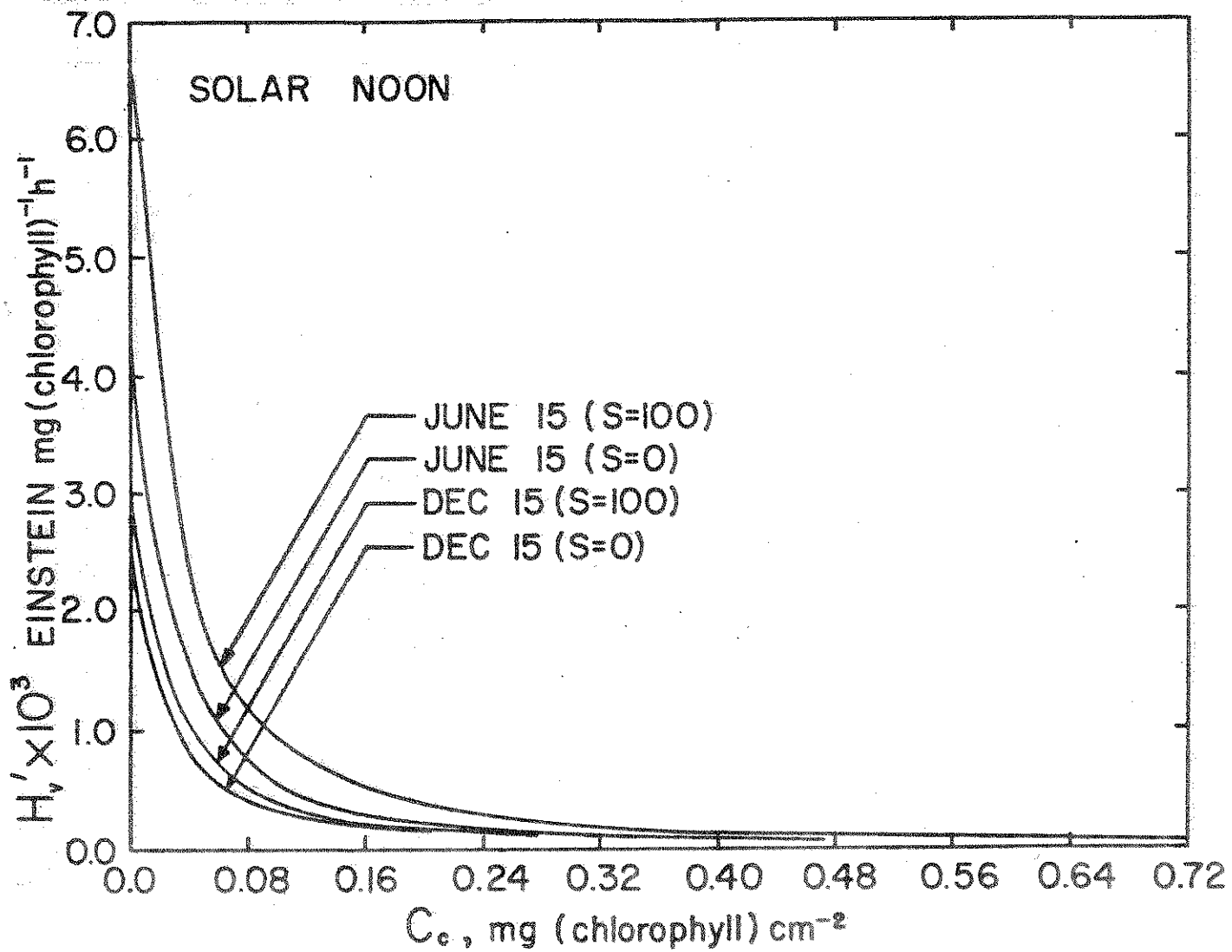

Figure 15. Radiation absorption per unit mass of chlorophyll as a function of integrated chlorophyll concentration at solar noon on June 15 and December 15.

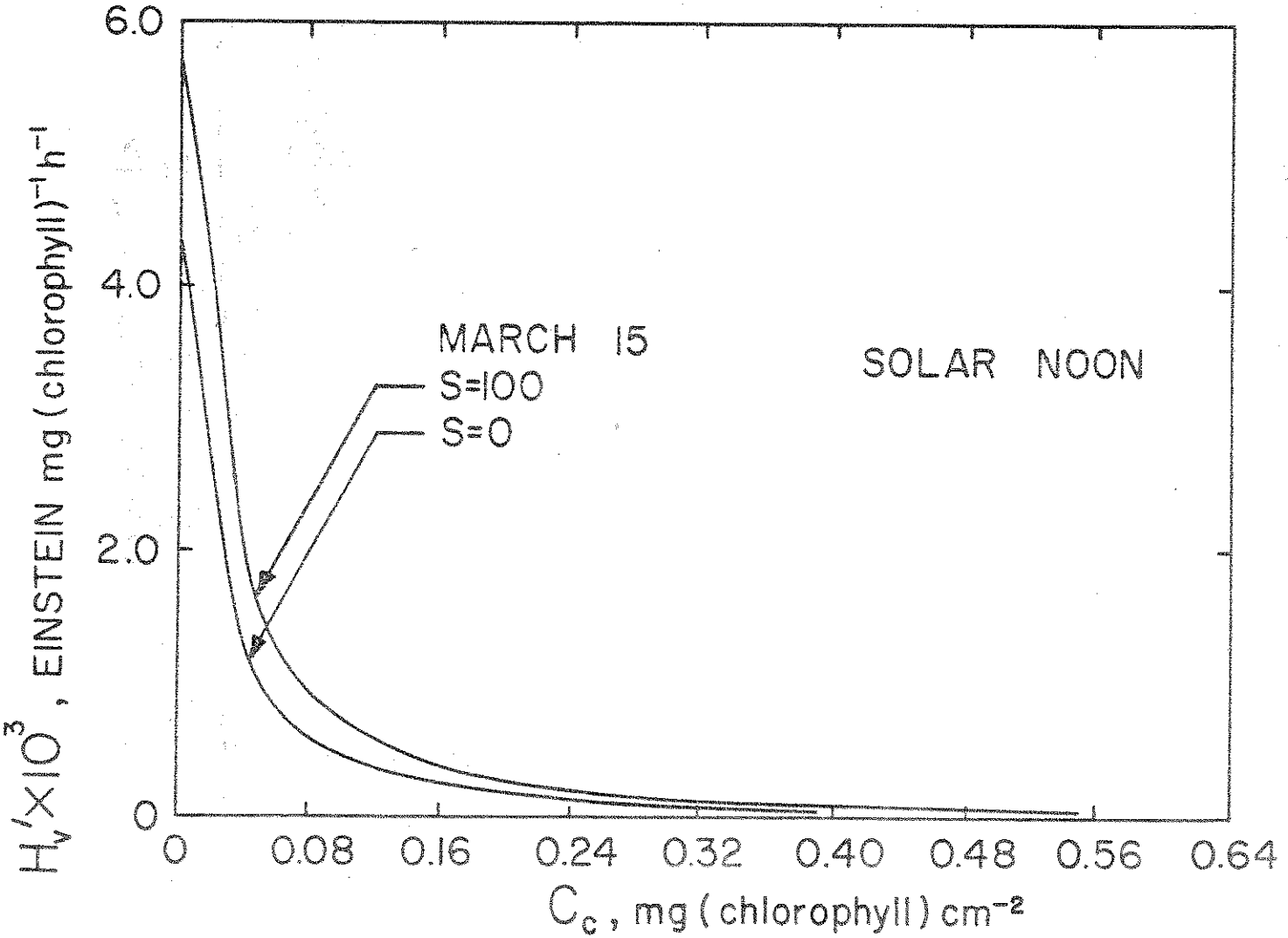

Figure 16. Radiation absorption per unit mass of chlorophyll as a function of integrated chlorophyll concentration at solar noon on March 15.

For an algal culture of known concentration, C_a, and chlorophyll content, r_c, the figures may be used to obtain the radiation attenuation with depth. Algal concentrations typically range from 0.15 to 3 $mg \cdot cm^{-3}$ in the field [9,33] and from 0.5 to 5 $mg \cdot cm^{-3}$ in the laboratory [11]. Selecting values of $C_a = 1\ mg \cdot cm^{-3}$ and $r_c = 0.05$ [11], a representative value of $C_a r_c$ is then 0.05 $mg(chlorophyll) \cdot cm^{-3}$. Since the plotted results indicate that radiation attenuation is nearly complete for $C_c \leq 0.75\ mg(chlorophyll) \cdot cm^{-2}$, this condition would occur at a depth of 15 cm for $C_a r_c = 0.05$. The depth over which there is photosynthetic activity is, of course, larger during the summer months than in the winter months, and it increases with decreasing C_a or r_c. For the range $0.15 \leq C_a \leq 5\ mg \cdot cm^{-3}$, this depth would vary from approximately 100 to 3 cm. These results are compatible with those reported in the literature for basins which have been used in the mass culture of algae. The depths typically range from 5 to 45 cm [2,9].

4.3 Oxygen and Algal Biomass Production

The foregoing radiation results have been used to predict the local rate of oxygen and algal biomass production within the pond, and the results are presented in Figs. 17 to 20 for the solar noon condition. The results in Figs. 17 and 18 pertain to the local net oxygen production P'_O, which is defined as

$$P'_O = R - U/r_c \tag{59}$$

and those in Figs. 19 and 20 pertain to the local net algal biomass production P'_a, which is defined as

$$P'_a = p_a/r_c C_a \tag{60}$$

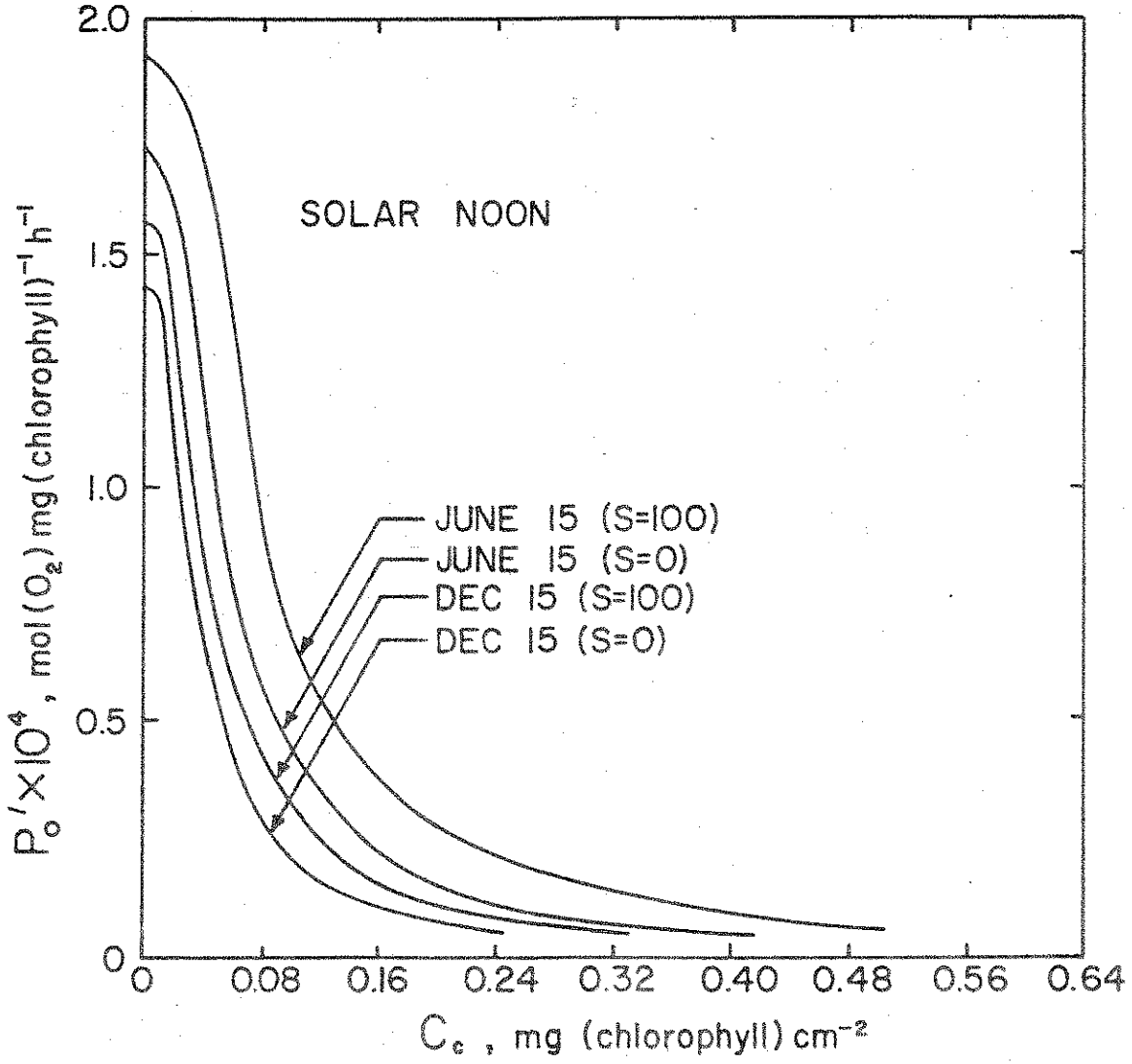

Figure 17. Oxygen production as a function of integrated chlorophyll concentration at solar noon on June 15 and December 15.

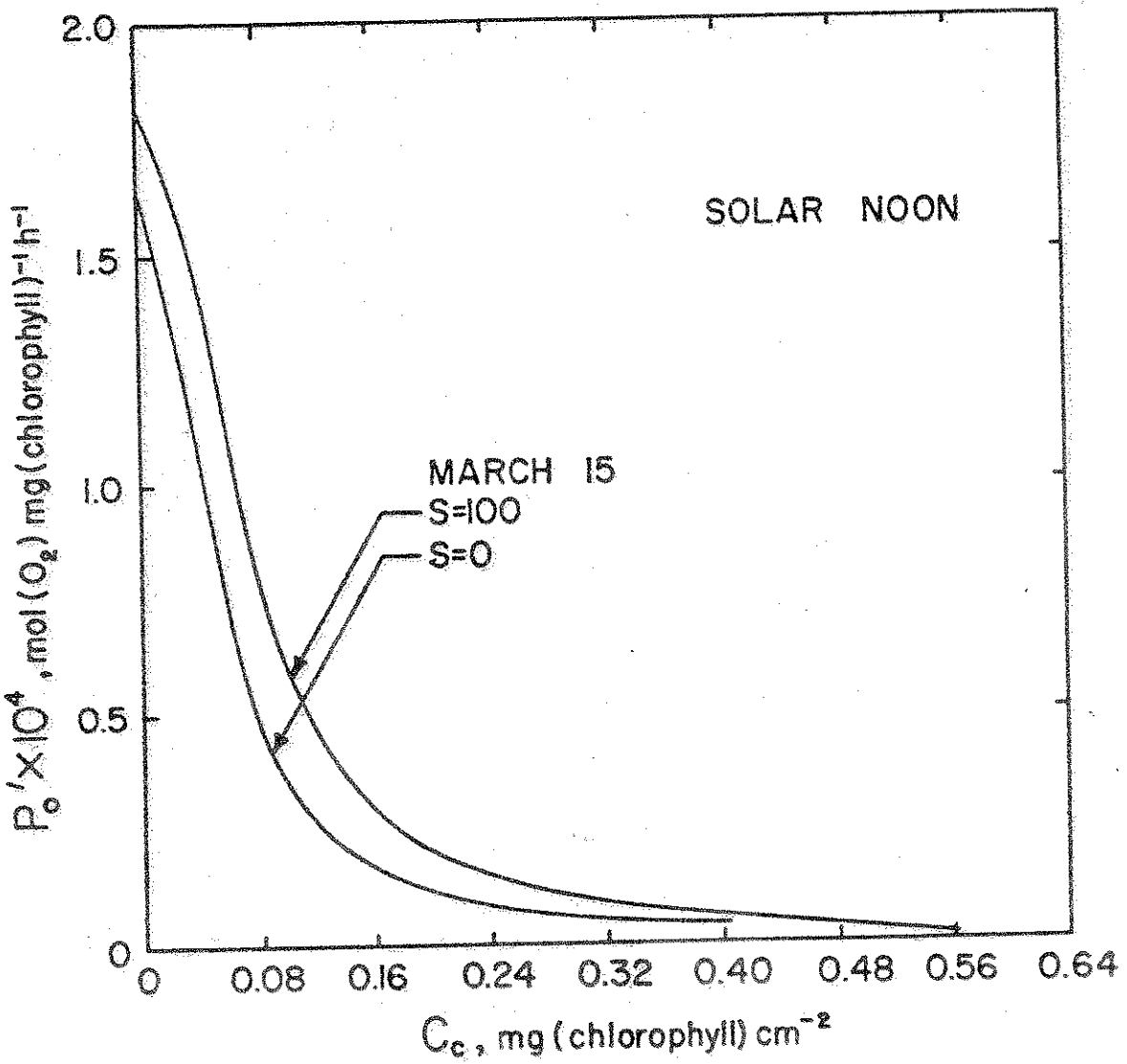

Figure 18. Oxygen production as a function of integrated chlorophyll concentration at solar noon on March 15.

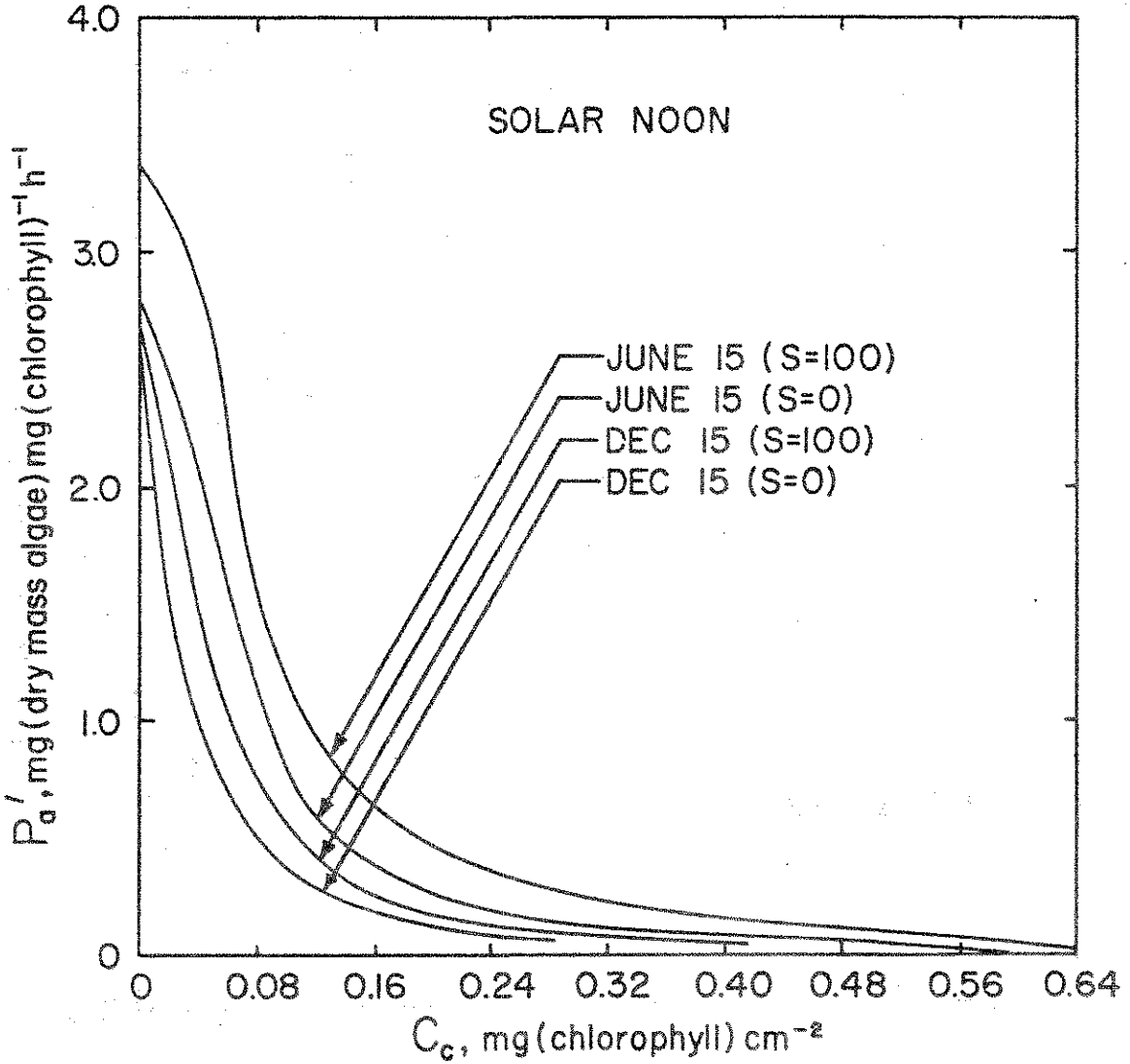

Figure 19. Algal biomass production as a function of integrated chlorophyll concentration at solar noon on June 15 and December 15.

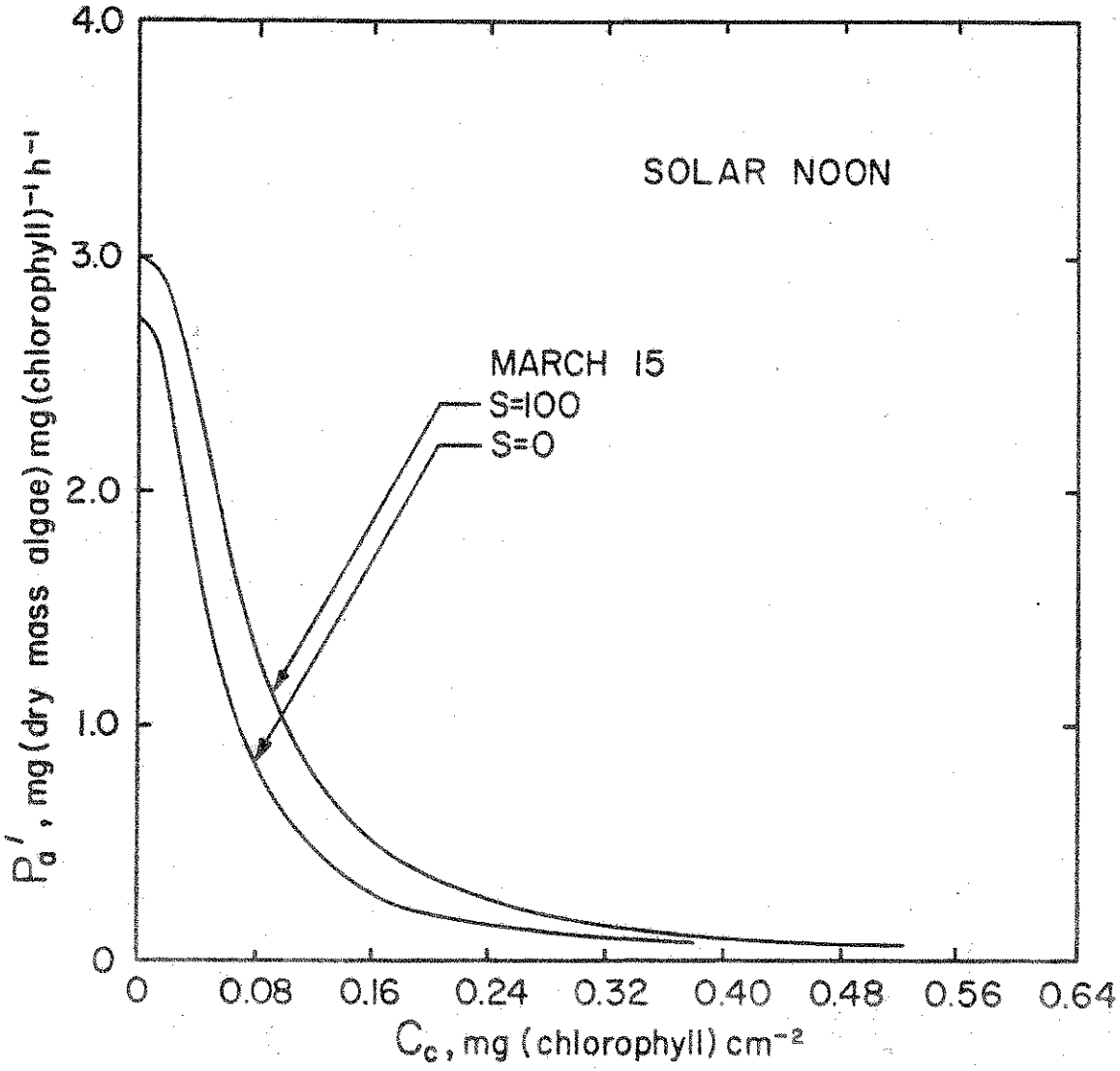

Figure 20. Algal biomass production as a function of integrated chlorophyll concentration at solar noon on March 15.

It is evident that oxygen and algal biomass production also fall off significantly with increasing C_c, with production being negligible for $C_c \leq 0.75$. However, it should be noted that in the surface layers the differences between production rates are not as large as the differences in the radiation field. For example, although H_v' for clear skies in June exceeds the value for clear skies in December by almost 100%, the difference in production rates is only approximately 25%. This condition is due to the fact that the photosynthetic apparatus is light saturated, or nearly light saturated, in the upper layers of the culture. The effects are, of course, more pronounced in June than in December. Light saturation effects are also manifested by the reduction in $|dP'/dC_c|$ with decreasing C_c, which is characteristic of the surface layers.

For any hour of the day, the local production rate may be integrated over C_c ($o \leq C_c \leq \infty$) to obtain the total production rate per unit pond surface area. Such integrations were performed for the daylight hours associated with March 15, June 15 and December 15, and the results are plotted in Figs. 21 through 24. The area under a particular distribution corresponds to the daily production per unit pond surface area, and the results obtained for the designated days are summarized in Table 1. Note that these results pertain only to net production for the daylight hours, and no attempt has been made to account for losses associated with dark respiration.

The results of Table 1 are in reasonable agreement with data which has been obtained for both laboratory and mass cultures. Dabes [11] reports a maximum algal biomass production of 32.5 $g \cdot d^{-1} \cdot m^{-2}$ for C. pyrenoidosa under laboratory conditions. This result is consistent with the predicted yield for June 15 under clear skies. Moreover, from results obtained for a 2/3 acre mass culture, Oswald and Golueke [8] report a daily oxygen yield of approximately

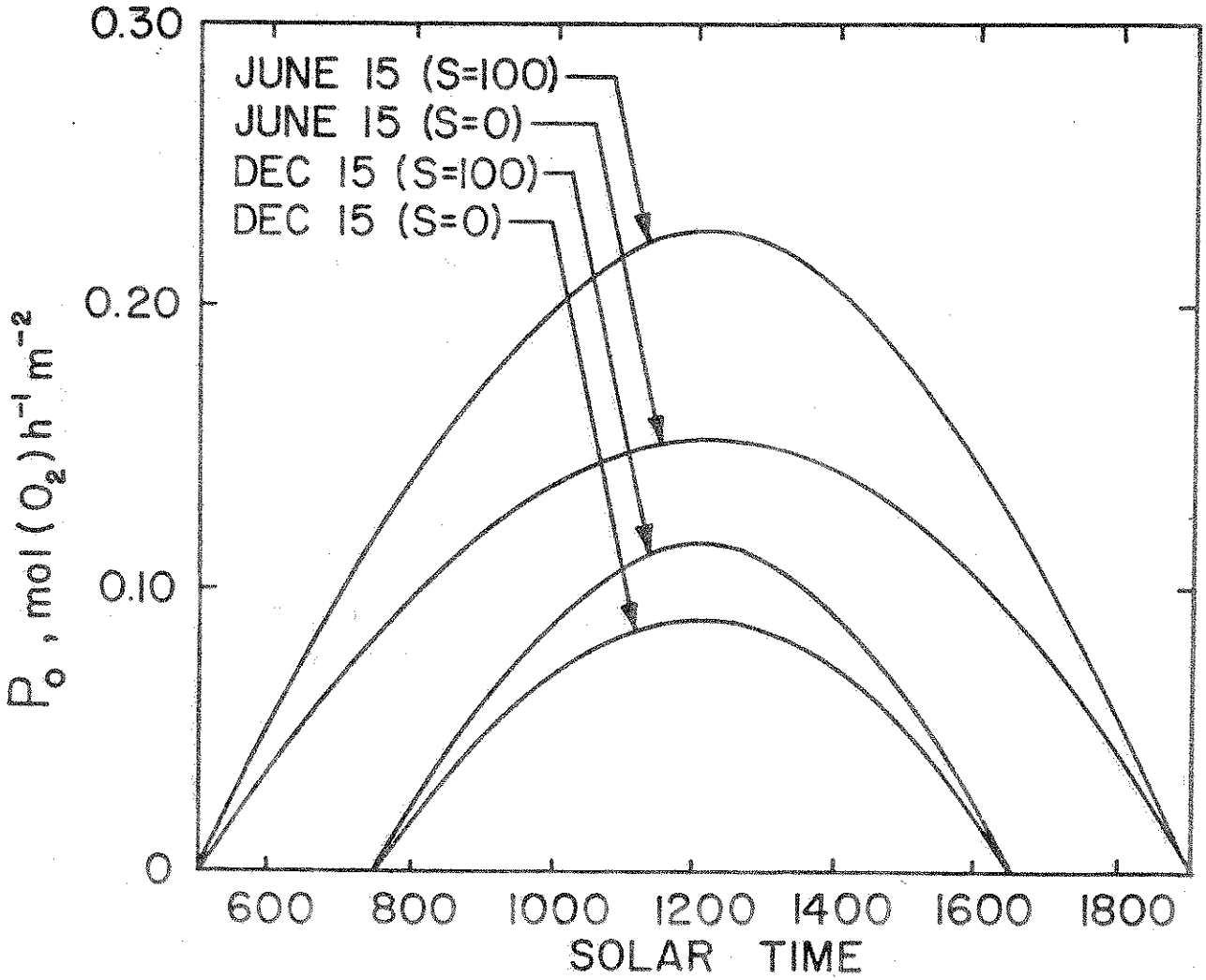

Figure 21. Hourly variation in oxygen production per unit surface area for June 15 and December 15.

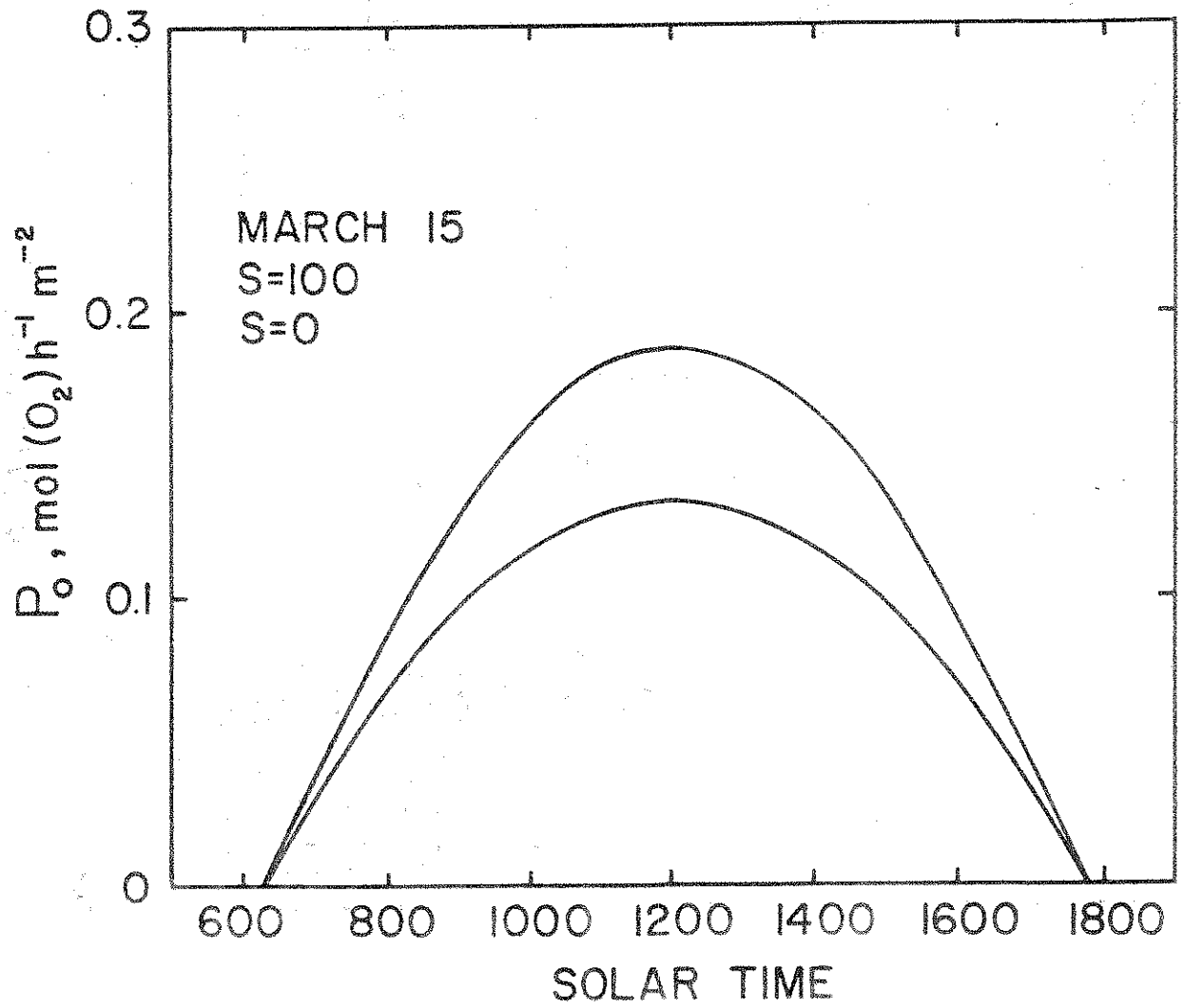

Figure 22. Hourly variation in oxygen production per unit surface area for March 15.

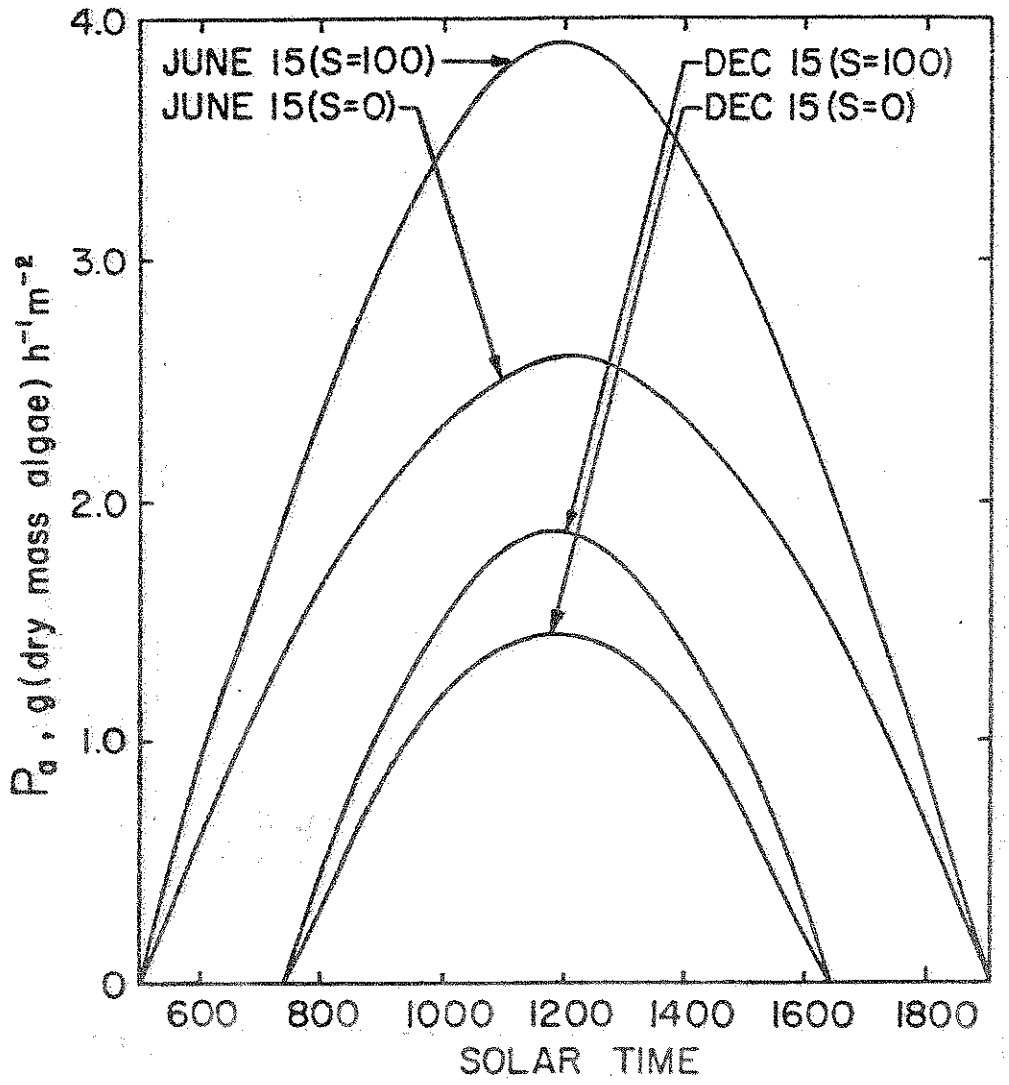

Figure 23. Hourly variation in algal biomass production per unit surface area for June 15 and December 15.

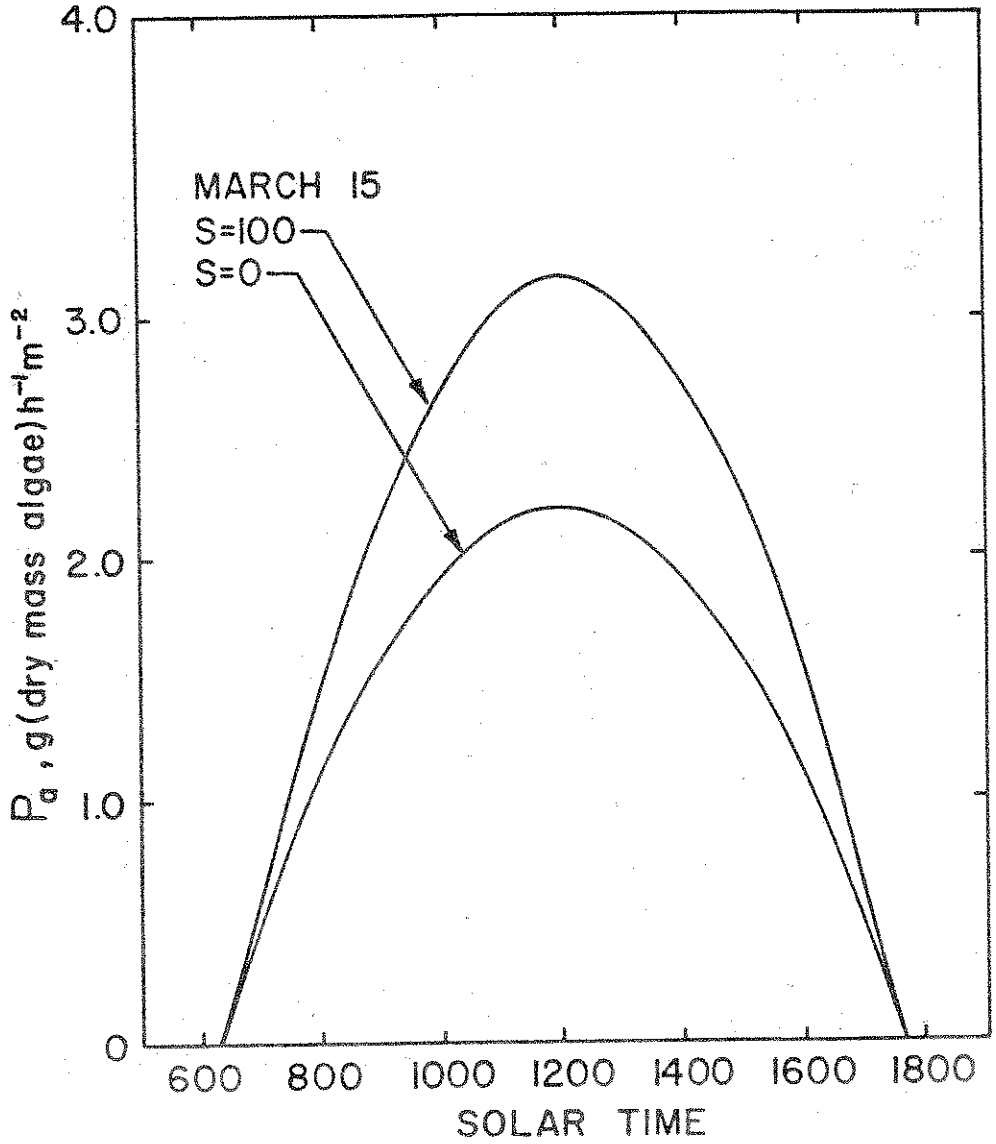

Figure 24. Hourly variation in algal biomass production per unit surface area for March 15.

Table 1. Daily oxygen and algal biomass production

	THIS STUDY		OSWALD [2]	
	$\overline{P_a}$	$\overline{P_O}$	$\overline{P_a}$	$\overline{P_O}$
	$g(\text{dry mass algae}) \cdot d^{-1} \cdot m^{-2}$	$mol(O_2) \cdot d^{-1} \cdot m^{-2}$	$g(\text{dry mass algae}) \cdot d^{-1} \cdot m^{-2}$	$mol(O_2) \cdot d^{-1} \cdot m^{-2}$
March 15				
(S=100)	23.02	1.369	15.21	0.793
(S=0)	16.60	0.993	7.98	0.416
June 15				
(S=100)	34.09	2.020	25.05	1.305
(S=0)	23.33	1.392	14.54	0.757
Dec. 15				
(S=100)	10.82	0.656	5.54	0.289
(S=0)	8.52	0.512	2.02	0.105

0.8 mol(O_2)$\cdot d^{-1}\cdot m^{-2}$. More recently Oswald [2] has reported yields for experimental ponds at 37° N latitude which are in the range $6 \lesssim \bar{P}_a \lesssim 25$ g$\cdot d^{-1}\cdot m^{-2}$ and $0.30 \lesssim \bar{P}_O \lesssim 1.30$ mol$\cdot d^{-1}\cdot m^{-2}$. He has also recommended use of the following correlations for predicting algal biomass and oxygen production

$$\bar{P}_a = 1.681 \times 10^{-2} \eta_v F_v \tag{61}$$

$$\bar{P}_O = 8.757 \times 10^{-4} \eta_v F_v \tag{62}$$

where η_v(%) is the efficiency for conversion of visible solar radiation to algal biomass and F_v(cal$\cdot d^{-1}\cdot cm^{-2}$) is the daily solar irradiance for the visible region of the spectrum. Using representative insolation data provided by Oswald [2] for 40°N latitude, yields were calculated from the above correlations, and the results are summarized in Table 1 for the months of interest. In addition Tamiya [1] has reported yields of approximately 20 g$\cdot d^{-1}\cdot m^{-2}$ for mass cultures of C. pyrenoidosa (TX 71105), and Boersma [9], summarizing the results of other investigators, reported yields of 10 to 33 g$\cdot d^{-1}\cdot m^{-2}$ for Scenedesmus under field conditions. More recently, Boersma [34] reported yields of up to 25 g$\cdot d^{-1}\cdot m^{-2}$ for C. vulgaris (211/8K) grown in fresh swine manure and indicated that yields of up to 30 g$\cdot d^{-1}\cdot m^{-2}$ may be attained.

The foregoing comparisons suggest that the model of this study is well suited for predicting the maximum possible yield which could be expected under field conditions. The measurements are generally lower than the predictions, but the comparisons suggest that, if growth conditions are optimized, actual yields will approach those predicted by the model. It is certainly reasonable to attribute the differences between actual and predicted yields to the existence of several rate limiting factors under field conditions. That is, nutrient concentrations and temperature,

as well as the solar irradiance, are likely to be limiting the photosynthesis rate under field conditions. In contrast the model of this study assumes that the only limitation is due to the solar irradiance. If efforts are made to optimize growth conditions in the field (through nutrient and temperature control), it would be reasonable to expect yields which are in good agreement with those obtained from the model.

The results of this study have also been used to compute the efficiency for conversion of solar radiation to algal biomass, and hourly variations are presented in Figures 25 and 26. The results are based on an assumed energy content of 5.5 kcal/g for the algal biomass, and the efficiency η_t is based upon the total solar irradiance. To convert to an efficiency based upon the solar irradiance for the PhAR, η_t should be divided by 0.45, the approximate fraction of the total solar radiation which is in the PhAR [35]. That is, $\eta_v \sim \eta_t/0.45$.

A number of expected trends are revealed by the results of Figures 25 and 26. Consider the clear sky condition (S=100) for June 15 (Fig. 25). The comparatively low value of η_t and the flatness of the curve over most of the daylight hours may be attributed to light saturation effects in the upper layers of the pond. This effect is most significant when the solar irradiance is large (clear skies in the summer). The peak value of η_t, which occurs in the early morning and late afternoon, is therefore associated with reduced (nonsaturating) values of the solar irradiance. However, this peak efficiency is reduced by the fact that the reflectivity of the air-water interface increases with increasing solar zenith angle. The rapid decay of η_t to zero in the early morning and late afternoon is due to a significant increase in this reflectivity. Similar trends are revealed by the results for cloudy skies (S=0). Starting with the early morning condition, η_t increases rapidly due to a

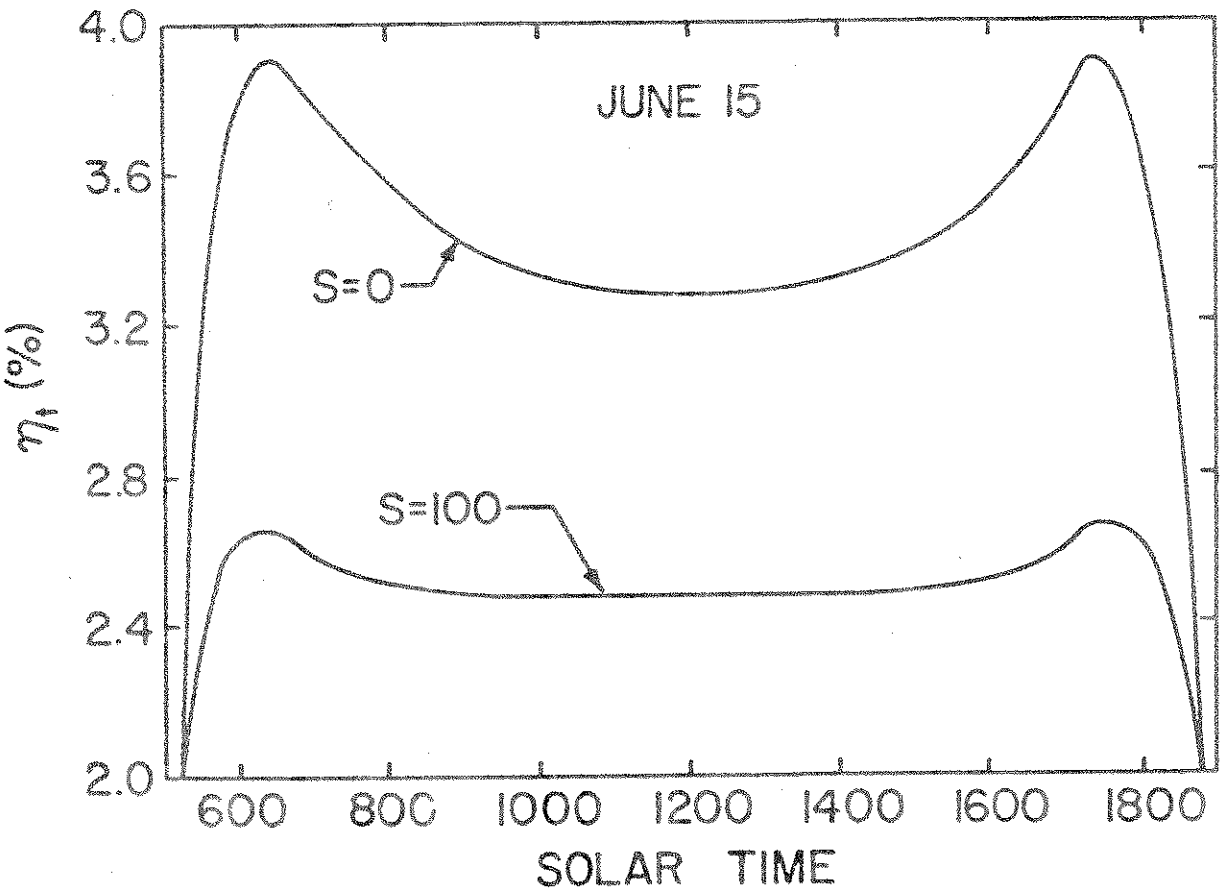

Figure 25. Hourly variation in the solar radiation conversion efficiency for June 15.

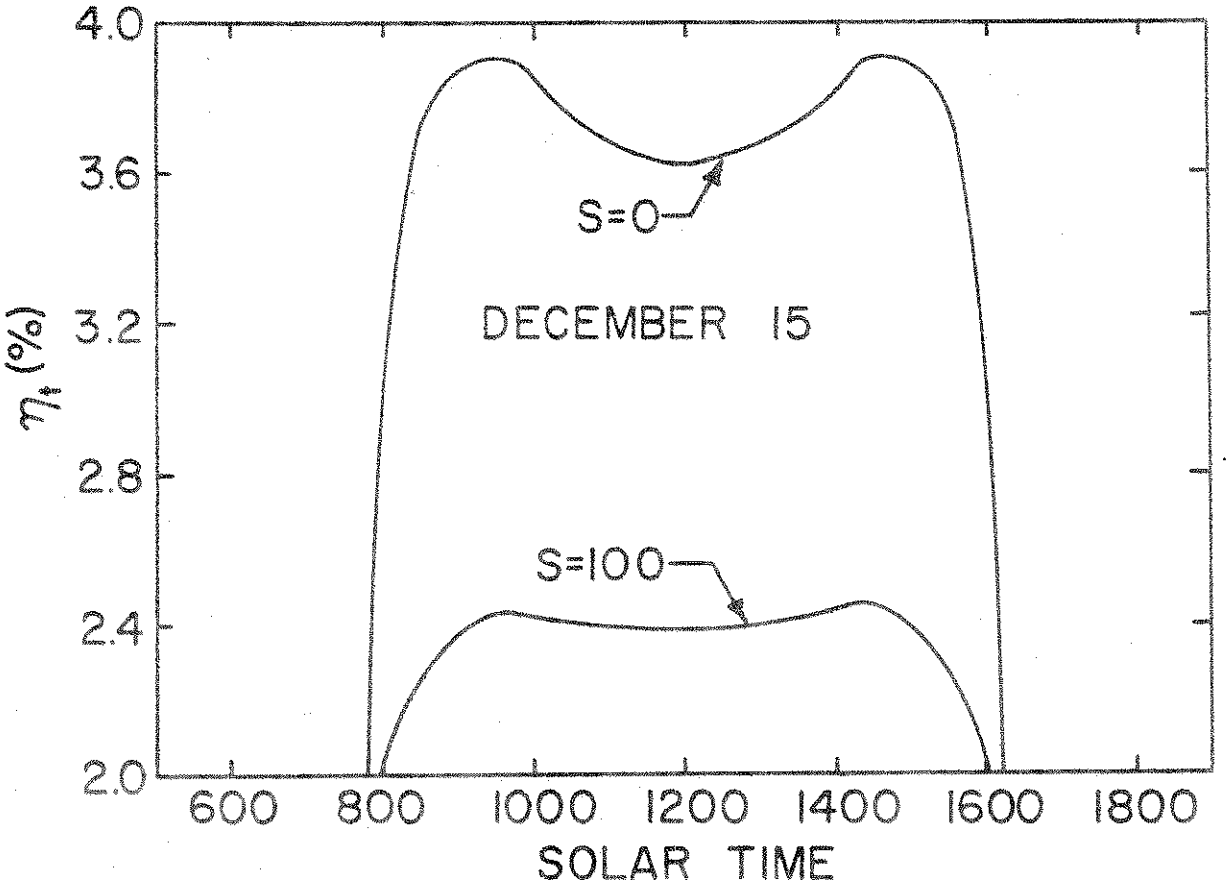

Figure 26. Hourly variation in the solar radiation conversion efficiency for December 15.

sharp decrease in the surface reflectivity with decreasing θ_i^c. However, the efficiency reaches a maximum due to the onset of light saturation and subsequently decreases due to the increasing importance of this effect. The trend is reversed following solar noon. Note that the larger values of η_t associated with S=0 (compared with S=100) may be attributed to the smaller values of the solar irradiance. However, although cloudy skies provide for larger conversion efficiencies, they still produce lower yields. Similar trends are revealed by the results for December 15 (Fig. 26), with the values of η_t being slightly higher than those for June 15. This trend may be attributed to the reduction in solar irradiance associated with winter conditions.

It should be noted that the calculations of this study suggest that a maximum efficiency of $\eta_t \sim 3.6\%$ ($\eta_v \sim 8.0$) may be achieved in the field (under cloudy skies). This efficiency is a good deal lower than the maximum theoretical value of $\eta_v \sim 20\%$ [10], which would be achieved if all of the available PhAR could be used in the photosynthesis process. However, it is still higher than the values of $1 \leq \eta_v \leq 5\%$ which have been achieved in mass cultures. The efficiency under field conditions could be increased by maintaining suitable nutrient and temperature controls and by using certain thermophilic strains of algae which are characterized by high levels of light saturation.

To determine the yearly algal biomass or oxygen production, one need only sum the daily yield over the entire year. In this study daily yields were calculated for the 15th day of each month for both the S=0 and S=100 conditions. In addition, from climatological data for Indianapolis, Indiana during the year 1974, an average value of the percent sunshine ($\bar{S}$) has been obtained for each of the twelve months. Daily yields were then calculated for the 15th day of each month, assuming that cloud cover effects could be approximated by using the value of $\bar{S}$ for the month. The results are pre-

sented in Table 2 and Figures 27 through 29. The S=100 and S=0 conditions provide upper and lower limits associated with the availability of solar radiation, and the $\bar{S}$ condition provides an approximation to actual conditions for the year 1974. Yields are, of course, higher during the summer months due to the higher values of the solar irradiance, and the conversion efficiency is lower for the same reason. The yields listed at the bottom of Table 2 represent integrated values for the entire year. The values corresponding to $\bar{S}$ are thought to provide a reasonable estimate of the yearly production which could be expected from a mass culture located in the midwest, provided that suitable temperature and nutrient controls are maintained.

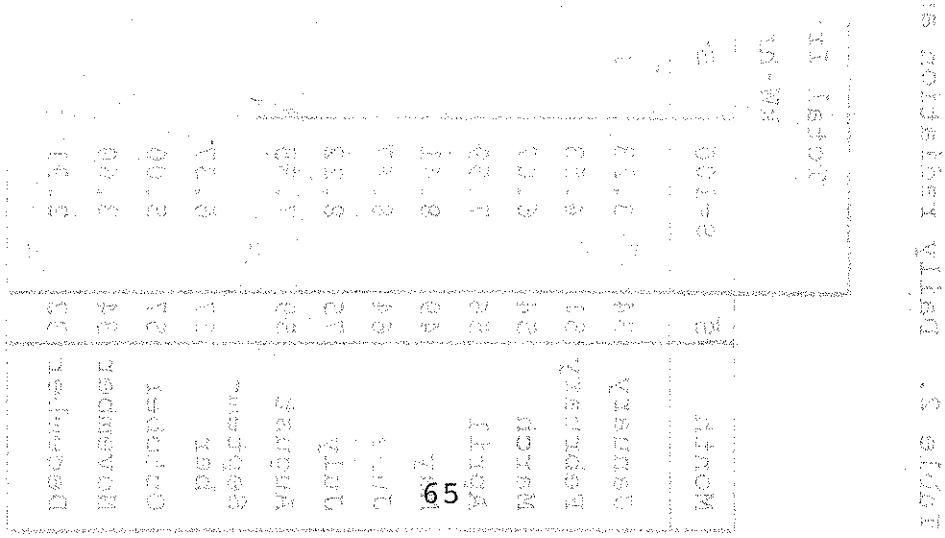

Table 2. Daily radiation and yields for the 15th day of each month (Indianapolis, Indiana).

		Total Irradiance $kW \cdot hr \cdot m^{-2} \cdot d^{-1}$			$\bar{P}_a$ $g(\text{dry mass algae}) \cdot d^{-1} \cdot m^{-2}$			$\bar{P}_O$ $mol(O_2) \cdot d^{-1} \cdot m^{-2}$			
Month	$\bar{S}$	S=100	S=0	$S=\bar{S}$	S=100	S=0	$S=\bar{S}$	S=100	S=0	$S=\bar{S}$	η_t
January	34	3.23	1.61	2.16	11.95	9.20	10.13	0.715	0.553	0.608	0.030
February	51	4.53	2.27	3.42	16.94	12.76	14.89	1.011	0.765	0.890	0.028
March	54	6.07	3.04	4.68	23.02	16.60	20.07	1.369	0.993	1.196	0.027
April	56	7.59	3.79	5.92	29.00	20.47	25.23	1.719	1.222	1.500	0.027
May	49	8.41	4.21	6.27	32.71	22.56	27.53	1.940	1.346	1.637	0.028
June	64	8.67	4.34	7.11	34.09	23.33	30.21	2.020	1.392	1.794	0.027
July	75	8.22	4.11	7.19	32.71	22.25	30.10	1.939	1.328	1.786	0.027
August	59	7.35	3.68	5.84	29.35	20.06	25.54	1.743	1.198	1.520	0.028
September	57	6.37	3.19	5.00	24.81	17.45	21.65	1.475	1.043	1.289	0.028
October	57	5.00	2.50	3.93	19.09	13.98	15.32	1.138	0.837	1.009	0.028
November	34	3.60	1.80	2.41	13.63	10.33	11.45	0.815	0.620	0.686	0.030
December	32	2.91	1.46	1.92	10.82	8.52	9.26	0.656	0.512	0.558	0.031
					8.47	6.01	7.35	503.65	359.51	440.72	
					$kg(\text{dry mass algae}) \cdot yr^{-1} \cdot m^{-2}$			$mol(O_2) \cdot yr^{-1} \cdot m^{-2}$			

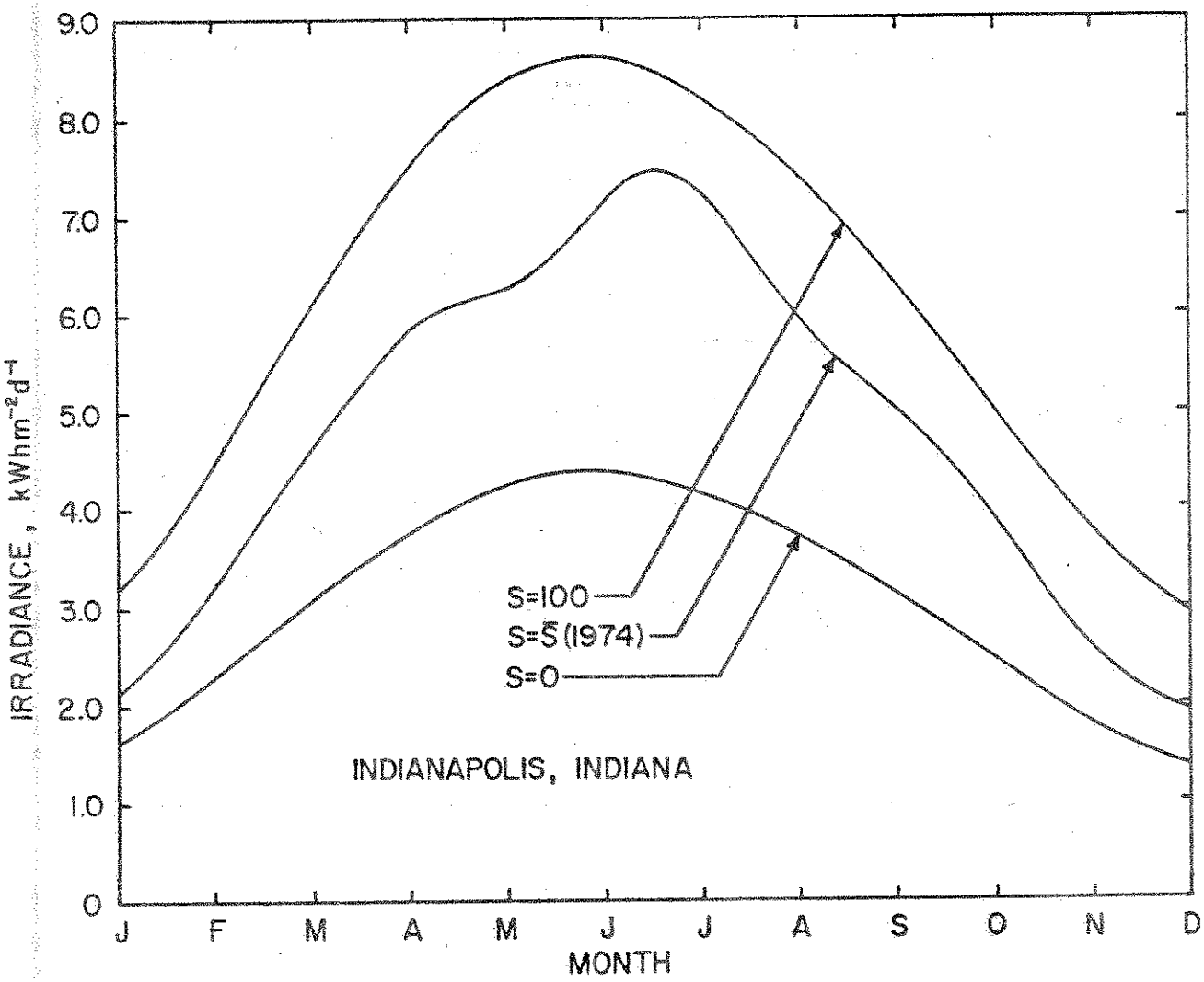

Figure 27. Daily irradiance as a function of time of year.

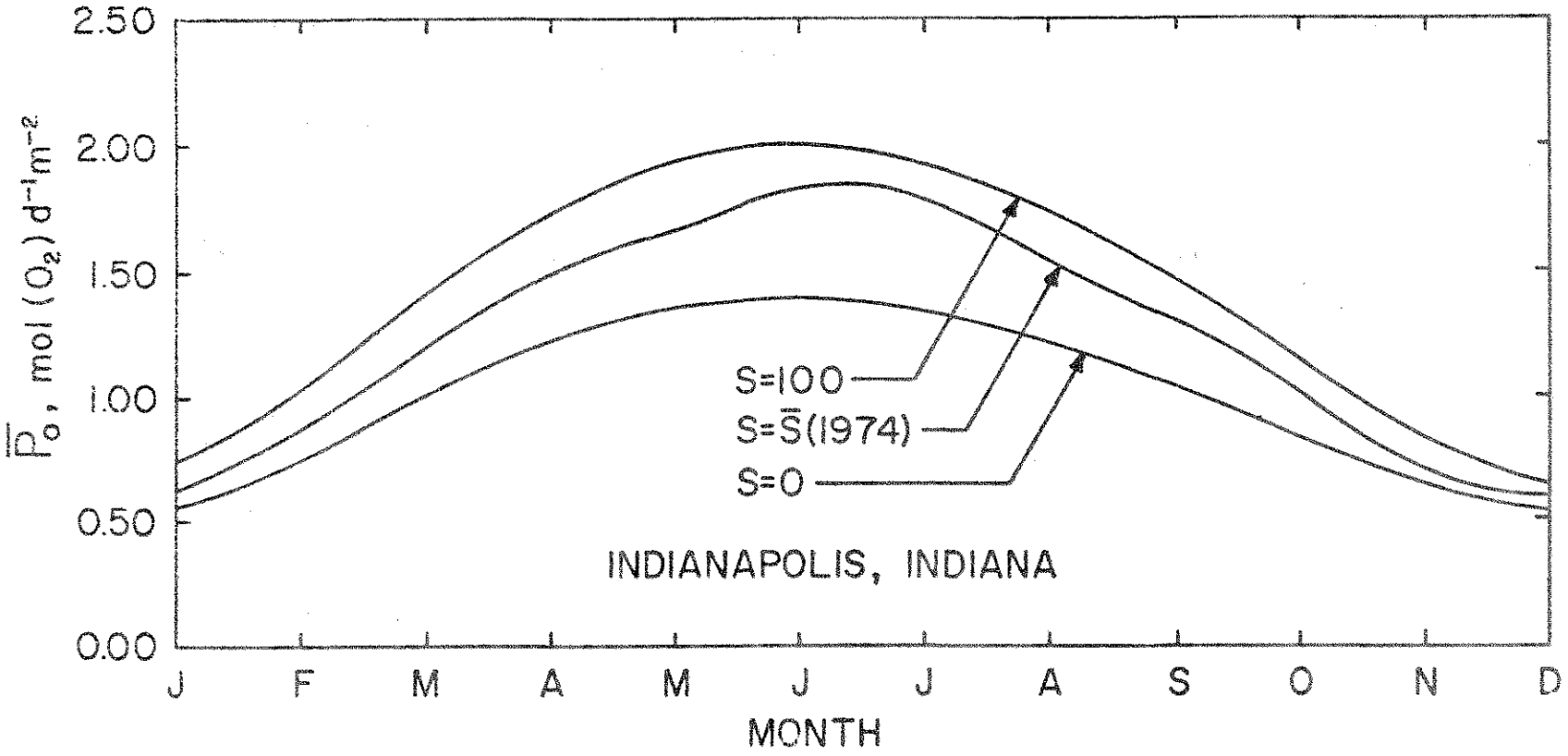

Figure 28. Daily oxygen production as a function of time of year.

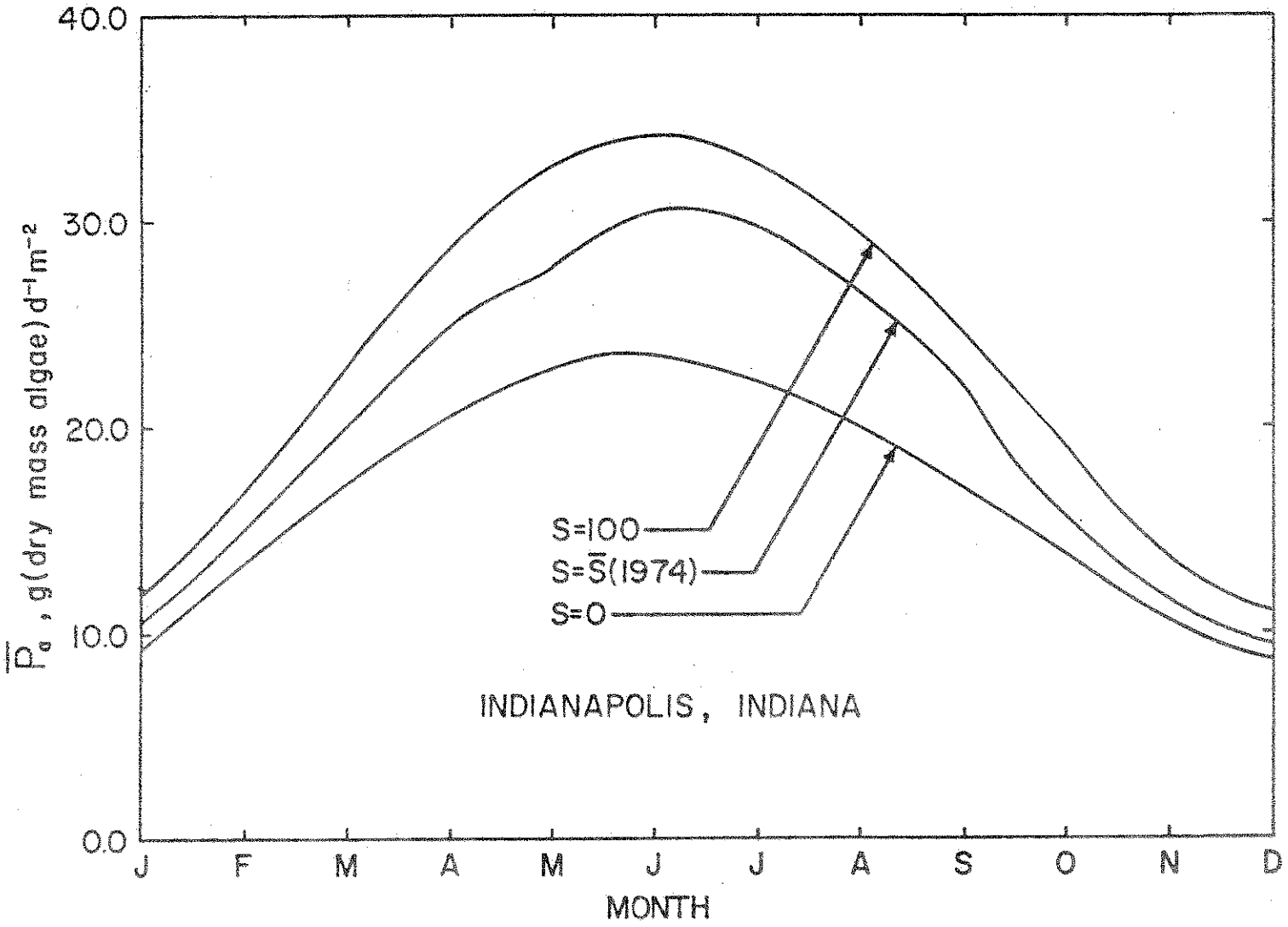

Figure 29. Daily algal biomass production as a function of time of year.

CHAPTER 5 SUMMARY

The purpose of this study has been to develop a reliable model for predicting the production of mass algal cultures. Efforts were focused on modeling the effects of variable solar irradiance, while limitations due to nonsaturating nutrient concentrations and nonoptimum temperatures were assumed to be negligible. A kinetic model was used which is consistent with the contemporary view of the photosynthesis process. Moreover the solar irradiance at the surface of the culture, as well as the radiation field within the culture, were determined using methods which are consistent with the underlying physics.

It is felt that the model may be used to obtain reasonable estimates of algal biomass and oxygen production under field conditions for which temperature and nutrient control are maintained. This assertion is based on the fact that daily yield predictions obtained from the model are in good agreement with maximum yields which have either been measured or inferred from field studies. The model therefore provides a useful tool for estimating the diurnal and seasonal performance of a mass culture for different geographic locations. It may also be a useful aid in the interpretation of field data and in determining optimum design and operating conditions.

The major uncertainties related to use of the model are not inherent in the underlying assumptions. They are due, instead, to uncertainties in required input parameters. There is certainly reason to question the accuracy of published data concerning the solar irradiance and the influence of cloud coverage on the collimated and diffuse components. In addition, due to limited information on the directional distribution of the diffuse radiation, there is considerable uncertainty concerning the nature of this distribution.

Finally, little has been done to accurately determine the inherent optical properties for the various species of unicellular algae, particularly for cultures representative of field conditions. However, as improvements in the foregoing data base become available, they may be readily incorporated into the present model.

REFERENCES

1. H. Tamiya, Mass culture of algae. Ann. Rev. Plant Physiol. 8, 309 (1957).

2. W.J. Oswald, Productivity of algae in sewage disposal. Solar Energy 15, 107 (1973).

3. J.F. Gordon, Algal proteins and the human diet. In Proteins as Human Food (R.A. Lawrie, editor), p. 328. Avi Publishing Co. (1970).

4. C.J. Soeder and W. Pabst, Gesichtspunkte für die Verwendung von Mikroalgen in der Ernährung von Mensch und Tier. Ber. Deutsch. Bot. Ges. 83, 607 (1970).

5. B. Volesky, J.E. Zajic and E. Knettig, Algal products. In Properties and Products of Algae (J.E. Zajic, editor), p. 49, Plenum Press, New York (1970).

6. W.J. Oswald and C.J. Golueke, Biological transformation of solar energy. Adv. Appl. Microbiol. 2, 232 (1960).

7. W.J. Oswald, Solar energy fixation with algal-bacterial systems. Presented at the Conference on Biological Transformation of Solar Energy, Bethesda, Maryland, September (1973).

8. W.J. Oswald and C.J. Golueke, Harvesting and processing of wastegrown microalgae. In Algae, Man and Environment (D.F. Jackson, editor), p. 371, Syracuse Univ. Press, Syracuse, New York (1968).

9. L.L. Boersma et al., Animal waste conversion systems based on thermal discharges. Rep. 416, Agricultural Experiment Station, Oregon State University, September (1974).

10. J. Meyers, Algal culture. In Encyclopedia of Chemical Technology (R.E. Kirk and D.F. Othmer, editors), p. 649, Interscience Publishing, New York (1971).

11. J.N. Dabes, C.R. Wilkie and K.H. Sauer, The behavior of Chlorella pyrenoidosa in steady state continuous culture. Lawrence Radiation Laboratory, Univ. California, Berkeley, August (1970).

12. G. Shelef, W.J. Oswald and C.G. Golueke, Kinetics of algal systems in waste treatment. SERL Rep. No. 68-4,

Sanitary Engineering Research Laboratory, Univ. of California, Berkeley, May (1968).

13. C. Sorokin, Calefaction and phytoplankton. Bioscience 28, 1153 (1971).

14. W.J. Oswald, Ecological management of thermal discharges. J. Environ. Qual. 2, 302 (1973).

15. J.G. Knudsen and L.L. Boersma, Future development in waste heat utilization. Circular No. 49, Agricultural Experiment Station, Oregon State University, September (1975).

16. W.J. Oswald and H.B. Gotaas, Photosynthesis in waste treatment. Transactions of Amer. Soc. Civil Engrs. 122, 73 (1957).

17. C. Sorokin and R.W. Krauss, Effects of temperature and illuminance on Chlorella growth uncoupled from cell division. Plant Physiol. 37, 37 (1962).

18. J.L.P. van Oorschot, Conversion of light energy in algal culture. Mededel. Landbouwhogeschool Wageningen 55, 255 (1955).

19. B. Kok, Photosynthesis in flashing light. Biochem. Biophysiol. Acta 21, 245 (1956).

20. J.L. Threlkeld, Thermal Environmental Engineering, 2nd edition, Prentice-Hall, Inc., Englewood Cliffs, N.J. (1970).

21. I.N. Yaroslavtzev, Distribution of the energetical and light intensity of diffuse atmospheric radiation over the celestial sphere. Bulletin of Leningrad University, No. 5 (1953).

22. S. Chandrasekhar, Radiative Transfer, Dover Publications, Inc. (1960).

23. K. Ya. Kondratyev, Radiation in the Atmosphere, Academic Press, New York (1969).

24. N. Robinson, Solar Radiation, Elsevier Publishing Co., New York (1966).

25. P.P. Paily, E.O. Macagno and J.F. Kennedy,Winter-regime surface heat loss from heated streams. IIHR Rep. No. 155, Univ. Iowa, Iowa City, (1974).

26. B.M. Duggar, Biological Effects of Radiation, Vol. 2, McGraw-Hill, New York (1936).

27. Local Climatological Data, National Climatic Center, U.S. Dept. of Commerce, Asheville, N.C.

28. H.H. Kimball, Measurements of solar radiation intensity and determination of its depletion by the atmosphere. Monthly Weather Review 58 (1930).

29. S.J. Bolsenga, Daily sums of global radiation for cloudless skies. Res. Rep. 160, U.S. Army Cold Regions Research and Engineering Laboratory, Hanover, N.H. (1964).

30. R. Siegel and J.R. Howell, Thermal Radiation Heat Transfer, McGraw-Hill, Inc., New York (1972).

31. Anonymous, Standard procedures to compute atmospheric radiative transfer in a scattering atmosphere. Report of the Radiation Commission of the International Association of Meteorology and Atmospheric Physics (1973).

32. K.J. Daniel and F.P. Incropera, A comparison of methods for predicting radiation absorption and scattering by solids suspended in water. TR No. ME-HTL-77-1, School of Mechanical Engineering, Purdue University (1977).

33. S.A. Hart and C.G. Golueke, Producing algae in lagoons. Trans. ASAE 8, 122 (1965).

34. L. Boersma et al., Protein production rates by algae using swine manure as substrate. In Energy, Agriculture and Waste Management (W.J. Jewell, editor), p. 475, Ann Arbor Science Publishing, Ann Arbor, Michigan (1975).

35. P. Moon, Proposed standard radiation curves for engineering use. J. Frank. Inst. 230, 583 (1940).

Water Resources Research Center
Lilly Hall of Life Sciences
Purdue University
West Lafayette, Indiana 47907